Chapter 8
Emerging Metal-Organic Framework Nanomaterials for Cancer Theranostics

Elham Asadian, Mahnaz Ahmadi, Rüstem Keçili, and Fatemeh Ghorbani-Bidkorbeh

Contents

E. Asadian
Department of Medical Physics and Biomedical Engineering, School of Medicine, Shahid Beheshti University of Medical Sciences, Tehran, Iran

M. Ahmadi · F. Ghorbani-Bidkorbeh (✉)
Department of Pharmaceutics, School of Pharmacy, Shahid Beheshti University of Medical Sciences, Tehran, Iran
e-mail: f.ghorbani@sbmu.ac.ir

R. Keçili
Yunus Emre Vocational School of Health Services, Department of Medical Services and Techniques, Anadolu University, Eskişehir, Turkey

M. Saravanan, H. Barabadi (eds.), *Cancer Nanotheranostics*, Nanotechnology in the Life Sciences, https://doi.org/10.1007/978-3-030-74330-7_8

List of Acronyms and Abbreviations

5-Fu	5-Fluorouracil
BDC	Benzene dicarboxylic acid
BTC	1,3,5-Benzenetricarboxylic acid (trimesic acid)
CD	Cyclodextrin
CDT	Chemodynamic therapy
CT	X-ray computed tomography
Cur	Curcumin
DEF	N,N-Diethylformamide
DMF	N,N-Dimethylformamide
DOX	Doxorubicin
EPR	Enhanced permeability and retention
FL	Fluorescence
HKUST	Hong Kong University of Science and Technology
IRMOF	Isoreticular metal-organic framework
LBL	Layer-by-layer
MIL	Material of Institute Lavoisier
MIm	2-Methylimidazole
MOFs	Metal-organic frameworks
MRI	Magnetic resonance imaging
MW	Microwave
MWCNTs	Multiwalled carbon nanotubes
NIR	Near infrared
nMOFs	NanoMOFs
NPs	Nanoparticles
PAI	Photoacoustic imaging
PB	Prussian blue
PCN	Porous coordination network
PDA	Polydopamine
PDT	Photodynamic therapy
PEG	Polyethylene glycol
PET	Positron emission tomography
Ppy	Polypyrrole
PS	Photosensitizer
PTT	Photothermal therapy
RhB	Rhodamine B
ROS	Reactive oxygen species
SAM	Self-assembled monolayer
TCPP	Tetrakis (4-carboxyphenyl) porphyrin
UiO	Universitetet i Oslo
ZIF	Zeolitic imidazolate framework

8.1 Introduction

Cancer, which is used as a generic term for a large group of diseases associated with the abnormal cell growth and subsequent invasion to other parts of the body, is one of the major public health threats and accounts for millions of deaths worldwide. Two main challenges concerning cancer diagnosis and treatment correspond to the (1) late diagnosis of the disease due to the lack of early symptoms which resulted in spread to other sites in the body (metastasis) and (2) nonspecific distribution of highly toxic chemotherapeutic drugs that affect normal tissues. On the other hand, agents which are used for diagnostic and therapeutic purposes come up with some limitations including low bioavailability, undesirable side effects, and rapid clearance from the body. Hence, designing novel strategies seems to be inevitable in order to address these challenges. In this regard, nanoparticle-based systems such as polymeric, magnetic, iron oxide, and gold nanoparticles are considered as intriguing candidates to overcome these problems (Peer et al., 2007; Cho et al., 2008; Huang & Lovell, 2017). Nanomaterials have been widely investigated for drug/cargo delivery owing to their small size, high surface area, and enhanced loading capacities along with improving pharmacokinetics and biocompatibility (Hossen et al., 2019; Alexis et al., 2008). They can be also exploited as carriers of targeting ligands to target a specific tissue and reduce the toxicity of the drug molecules by on-site control release mechanisms (Singh & Lillard, 2009; Petros & DeSimone, 2010). In addition to therapeutic applications, nanoparticles are advantageous as diagnostic agents for biomedical imaging. Nanoparticles, pristine or conjugated with diagnosis agents, can be traced and detected in the body and, therefore, provide us with the opportunity not only to develop the imaging modalities to assist with disease detection but also to investigate the biodistribution (Nune et al., 2009; Choi & Frangioni, 2010; Han et al., 2019). In the meantime, simultaneous integration of therapeutic potentials of nanoparticles with their diagnostic capabilities, named *theranostic* approaches, has been the subject of interest in the past few years (Huang & Lovell, 2017; Xie et al., 2010). In this regard, various kinds of nanomaterials such as polymeric (Qian et al., 2017; Indoria et al., 2020), gold (Guo et al., 2017; Gharatape & Salehi, 2017), magnetic (Yoo et al., 2011; Gul et al., 2019), carbon (Gupta et al., 2019), and iron oxide (Dadfar et al., 2019) nanoparticles have been widely used for theranostic applications. Among them, porous nanomaterials are of great importance due to their intrinsic properties as cargo carriers.

Metal-organic frameworks (MOFs), also called coordination polymers, are an emerging class of crystalline materials with uniform porous structure. Although they have been first discovered in 1965, the further development of MOFs was hampered by the collapse of their porous structure in the absence of solvent or other guest molecules (Yaghi et al., 1998; Kepert & Rosseinsky, 1999). In the late 1990s, Yaghi et al. reported on the synthesis of a highly stable metal-organic framework which maintained its crystallinity while fully desolvated and even after heating up to 300 °C (Li et al., 1999). Their simple and potentially universal synthetic route has opened up new horizons toward various design strategies which resulted in the

synthesis of more than 20,000 different MOFs with diverse size, morphology, and functionality within the past two decades.

MOFs are literally organic-inorganic hybrid materials composed of transition metal cations (or clusters) linked together by organic linkers through strong coordination bonds based on reticular chemistry (Fig. 8.1a). The versatility of organic building blocks and the diversity of metal-ligand combinations along with various adoptable synthesis methods have led to development of MOFs with structural flexibility. So far, a wide variety of MOFs with tunable chemical properties and ample functionalities have been prepared by different research groups, some of which are shown in Fig. 8.1b. As can be seen, the repetition of MOF building blocks forms a periodic cage-like framework with well-defined pore apertures where the pore size and structure can be controlled through wise choices of organic linkers (Lu et al., 2014).

MOF family possess fascinating properties stemmed from their unique structure such as extremely high specific surface area (up to 10,000 m^2g^{-1}), large pore volumes with well-defined pore aperture, tunable pore size, shape and dimensionality, and versatile functionality along with structural diversity. These superior

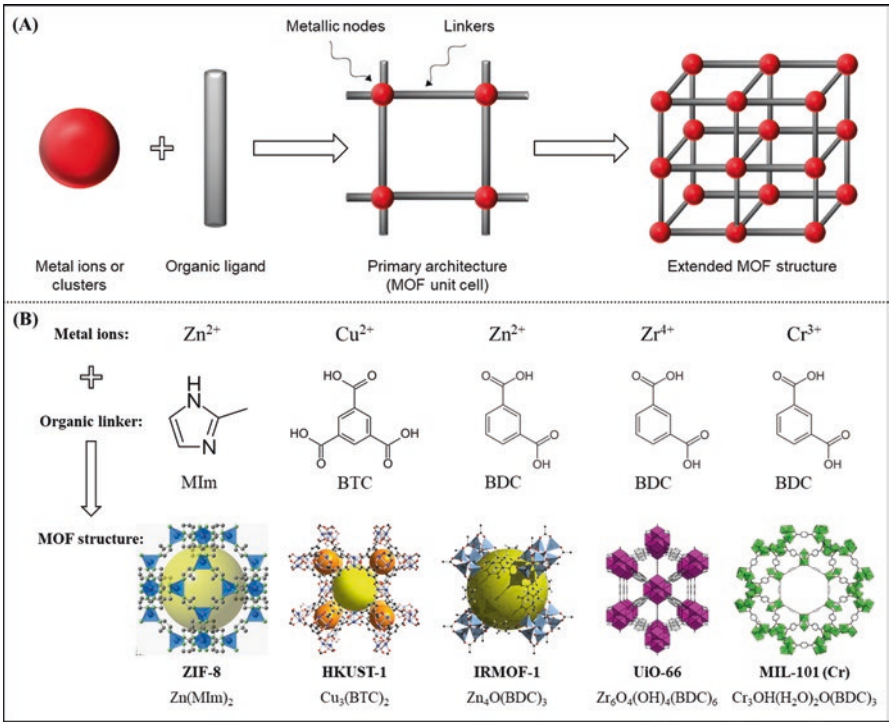

Fig. 8.1 (**a**) Schematic illustration of MOF structure composed of metallic nodes and organic linkers. (**b**) Some representative MOF structures (the yellow spheres represent the highest volume of the free pore in the structure)

characteristics turn them into potential candidates for a wide range of applications from gas storage, separation and purification (Li et al., 2018a; Xue et al., 2019a; Dhainaut et al., 2020), catalysis (Wang & Astruc, 2019; Zhu et al., 2020), and sensing (Kumar et al., 2015; Dolgopolova et al., 2018; Amini et al., 2020) to biomedical ones (Lu et al., 2018; Luo et al., 2019; Yang & Yang, 2020; Zhang et al., 2020). The fact that MOFs provide extremely high loading capacities as a result of their extraordinary porosities as well as their improved biocompatibility paves the way for their use as promising cargo delivery systems for drugs and therapeutic agents and even biomacromolecules such as proteins, genes, and nucleic acids (Wu & Yang, 2017; Cheng et al., 2018; Liu et al., 2019). On the other hand, MOFs are appealing candidates for biomedical imaging purposes (Della Rocca et al., 2011; Li et al., 2019a). They can be exploited as carriers for delivering imaging contrast agents or even serve as contrast agents themselves through appropriate selection of structural components. Moreover, the incorporation of superparamagnetic metal centers (i.e., Mn^{2+}, Fe^{3+}, and Gd^{3+}) in the framework makes it possible for the MR imaging applications. As a result, recent years have witnessed an increasing interest in the implementation of metal-organic frameworks as tools for cancer diagnosis and therapy (theranostics) by integrating their imaging and therapy capabilities into a single formulation (Cai et al., 2015; Zhao et al., 2016; Cai et al., 2017; Zhou et al., 2018; Pandey et al., 2020).

In the present chapter, the synthesis and modification methods of MOFs will be first addressed. Then, the therapeutic and imaging applications of MOFs will be highlighted. The next section will focus on nanoMOF-based theranostic platforms followed by the future perspectives toward the development of efficient theranostic systems.

8.2 MOF: Synthesis and Surface Modification

As mentioned previously, metal-organic frameworks are formed by the self-assembly of polynuclear metal clusters (named as "secondary building units, SBUs") and multitopic organic linkers as the structural key components and within the realm of reticular chemistry[1] (Kalmutzki et al., 2018). One of the fascinating features of MOFs is their synthetic flexibility, which allows the possibility of designing various kinds of topologies via rational choice of precursors. This capability makes it possible not only to control the pore size but also to regulate their internal environment. In addition to the structure and type of precursor used, the structural and functional tunability can be achieved by choosing the appropriate synthesis method along with controlling the synthetic parameters such as concentration of reagents, solvent polarity, temperature, pH of the solution, and the reaction time

[1] The term reticular derived from Latin *reticulum* which means "small net" and referred to the formation of an extended netlike structure through linking the molecular building blocks by means of strong coordination bonds.

(Meek et al., 2011; Stock & Biswas, 2012; Safaei et al., 2019; Al Amery et al., 2020). So far and as shown in Fig. 8.2, different synthetic approaches have been adopted to prepare MOFs with diverse morphologies which will be presented in the following sections.

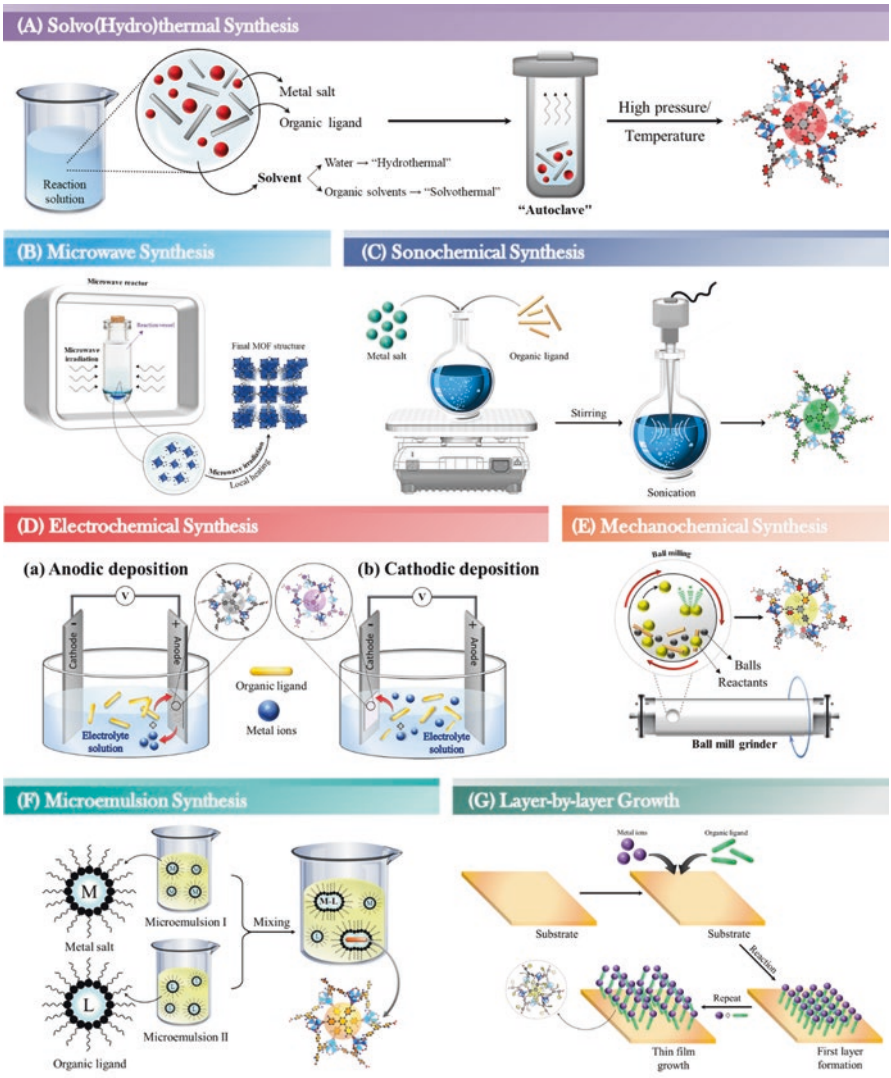

Fig. 8.2 Schematic representation of some synthetic methods widely applied for the preparation of MOF structures. (*The MOF crystal structures which relate to MOF-177 are adopted from Ref. Zhang et al. (2015) and only used as a schematic representative for MOFs prepared through various methods)

8.2.1 Direct Precipitation Reaction

Early efforts for producing MOFs have generally focused on low-temperature methods (Hoskins & Robson, 1990). These conventional techniques have been mainly relied on the simple mixing of the starting materials (i.e., metal salts and organic ligands) which have already been dissolved in suitable solvents followed by nucleation and crystal growth processes which finally result in precipitation of MOF structures. Once the precursors are mixed together and the critical nucleation concentration is exceeded, the initial nuclei are formed. The reaction solution will be then aged at constant low temperature (often room temperature) during which the solution mixture is concentrated by slow evaporation of the solvent and primary nuclei are consequently grown. As a result, tuning the reaction conditions, i.e., the rate of nucleation and growth processes, has a direct impact on controlling the size of the final product (Stock & Biswas, 2012; Rowsell & Yaghi, 2004). On the other hand, chemical and structural properties of the solvents including solubility, reactivity, polarity, dielectric constant, donor number, and the boiling point temperature play a key role in such liquid phase synthesis reactions (Al Amery et al., 2020). In the meantime, certain ligands contain functional groups (like carboxylic acid) which should be deprotonated prior to coordination, while so many polar solvents can compete with the organic linkers to coordinate with the available metal centers. Hence, the choice of solvent used is essential in achieving the desired MOF product. The direct precipitation approach has been utilized to prepare some prominent MOFs like MOF-5, MOF-74, MOF-177, MOF-199, and IRMOF-0 at room temperature (Tranchemontagne et al., 2008). It is noteworthy to mention that with this method, the MOF crystals not only can be synthesized in the solution phase but also can be grown on the surface of suitable substrates through nucleation and growth processes. For instance, ZIF-8 nanoparticles were synthesized on the surface of 3D graphene networks (Cao et al., 2014) or carbon cloth (Asadian et al., 2020) by immersing the substrate in methanolic solutions of $Zn(NO_3)_2$ and MIm for a specific period of time followed by thorough washing the substrate with appropriate solvent. The slow evaporation method is suitable for thermally sensitive starting materials; however when kinetically inert ions are used or in the case of MOFs with higher crystallinity degrees, high-temperature synthetic methods such as solvothermal/hydrothermal techniques are more desirable.

8.2.2 Solvothermal/Hydrothermal Synthesis

With the increasing tendency to synthesize MOF structures with improved crystallinity, techniques at higher operational temperatures became mandatory. In this regard, hydrothermal/solvothermal methods were found to be convenient synthetic routes. These techniques refer to the chemical reactions performed in a closed vessel at relatively high temperature (generally above the boiling point of solvent). In

the case of water as the solvent and when the reaction proceeds in an aqueous medium, the method is called "hydrothermal," while in "solvothermal" technique, the solvents used are non-aqueous (organic solvents). Regardless of the type of solvent, in both the aforementioned techniques, the reactants are first thoroughly dissolved in an appropriate solvent. The resulting homogeneous solution is then transferred to a Teflon lined stainless steel autoclave (Fig. 8.2a). Since the reaction proceeds at elevated temperature and in a sealed container, the pressure under which the MOF nanoparticles are formed is relatively high resulting in structures with higher degrees of crystallinity suitable for power X-ray diffraction (PXRD) analysis.

In 1995, Yaghi and Li proposed hydrothermal synthesis as a viable route to produce copper MOF with crystalline porous structure composed of extended channel network (Yaghi & Li, 1995). Their method involved exposing the reactants ($Cu(NO_3)_2 \cdot 2/5H_2O$, 4,4′-bpy and 1,3,5-triazine) to a specified temperature program in which the autoclave was kept at 140 °C for 24 h, then cooled to 90 °C, and held for 12 h followed by another 12 h at 70 °C and final cooling to the room temperature. Their results revealed that the hydrothermal conditions were essential to achieve the product as the same reaction did not succeed through refluxing even after 24 h. Although hydrothermal technique has been applied to synthesis certain kinds of MOFs (Chalati et al., 2011; Qian et al., 2012), its further implementation was hindered by poor water solubility of organic linkers and the stability issues of MOF structures in aqueous medium. From this respect, the solvothermal method is more convenient so that taking a glance at literature reveals that it is the most widely used technology for the synthesis of this family of nanomaterials (Park et al., 2006; Cheng et al., 2013; Sun et al., 2020; Hu et al., 2014; Esrafili et al., 2019; Xue et al., 2019b; Chen et al., 2020; Wang et al., 2019a). The solvents used in solvothermal synthesis could be protic such as ethanol, methanol, and acetic acid as well as aprotic ones like DMF (N,N-dimethylformamide), DEF (N,N-diethylformamide), and acetonitrile and should be carefully selected based on the polarity and dielectric constant to achieve the desired product.

Zeolitic imidazolate frameworks (ZIFs), as one of the most extensively studied subclasses of MOFs, are composed of tetrahedrally coordinated transition metal ions (i.e., Fe, Co, Cu, Zn) linked by imidazolate organic ligands. ZIFs borrowed their name from zeolites as a result of their zeolite-like topologies and integrate the advantages of their inorganic counterparts (namely, high chemical and thermal stability of zeolites) with those of MOF family (i.e., high porosity and surface area). Yaghi's group was the first to synthesize ZIF-8 using $Zn(NO_3)_2 \cdot 4H_2O$ and 2-methylimidazole (2-MIm) dissolved in DMF and via a solvothermal method at 140 °C (Park et al., 2006). The prepared ZIF-8 demonstrated high permanent porosity (1810 m^2/g) and extraordinary thermal rigidity (up to 550 °C) along with remarkable chemical stability (even in boiling alkaline aqueous solution and organic solvents).

The solvothermal technique has attracted a great deal of attention since it can be used to not only synthesize different types of MOFs but also provide us with the ability of tuning the size and morphology. The size and shape of MOF

nanostructures can be altered by varying the synthesis conditions including the type of solvents, the concentrations of reactants, and the presence of surfactants (Cheng et al., 2013; Sun et al., 2020; Hu et al., 2014; Esrafili et al., 2019). For instance, by controlling the degree of deprotonation of NH_2-BDC via adjusting the water content in a DMF-water mixed solvent system, Guo et al. synthesized a series of NH_2-MIL-53 (Al) crystals with different sizes and morphologies (Cheng et al., 2013). The results demonstrated the effect of water on modulating the nucleation and crystal growth process in such a way that differs the morphology from cube-like to rhomboid monocrystals. The same solvent-adjustment solvothermal strategy was also applied to prepare bimetallic NiCo frameworks (Sun et al., 2020). As shown in Fig. 8.3a, the size and shape of the resulting MOFs strongly depend on the composition of the solvent. It was revealed that the presence of water plays an important role in the formation of nanosheet-like structures by lowering the rate of ligand deprotonation and, as a consequent, the nucleation step. The concentration of the reactants is another critical parameter that affects the morphology during crystallization (Hu et al., 2014; Esrafili et al., 2019). Due to the crystalline structure of MOFs, changing the concentration of precursors as well as the presence of surfactants can orient their growth along specific crystal plates and, as a result, the formation of different morphologies.

Moreover, preparing MOF composites through combination of MOFs with various functional materials which are capable of introducing improved or rather novel properties has been the focus of interest during the past few years (Xue et al., 2019b; Chen et al., 2020). Considering the synthesis techniques of MOF-based composites, solvothermal method is regarded as a suitable approach in which the composite nanostructures can be achieved in a one-pot synthesis and through careful adjusting of the reaction conditions. As an example, Wang and coworkers introduced a flower-string-like NiCo MOF@MWCNT composites by utilizing carboxylated MWCNTs as a substrate for the in situ growth of binary NiCo MOF with the aid of solvothermal method (Wang et al., 2019a). The reaction proceeded in an autoclave by mixing $Ni(NO_3)_2{\cdot}6H_2O$, $Co(NO_3)_2{\cdot}6H_2O$, and 4,4′-biphenyldicarboxylic acid (BPDC) as organic ligand in a DMF-EtOH solution and in the presence of MWCNTs with different wt% (Fig. 8.3b). The MWCNTs not only act as a guiding agent on the MOF growth but also increase the conductivity of the composite material. In general, if the reaction parameters are properly controlled and, in the meantime, the nucleation process on the substrate and then the subsequent growth occur efficiently, MOF composites can be synthesized with high yield using a solvothermal method.

Nevertheless, the solvothermal technique generally requires long reaction times (from hours to weeks) at high temperatures and needs organic solvents which are toxic and pose environmental concerns. These challenges along with operational limitations (setup fabrication at large scale) are obstacles which should be addressed for scaling-up and commercialization of solvothermal synthesis.

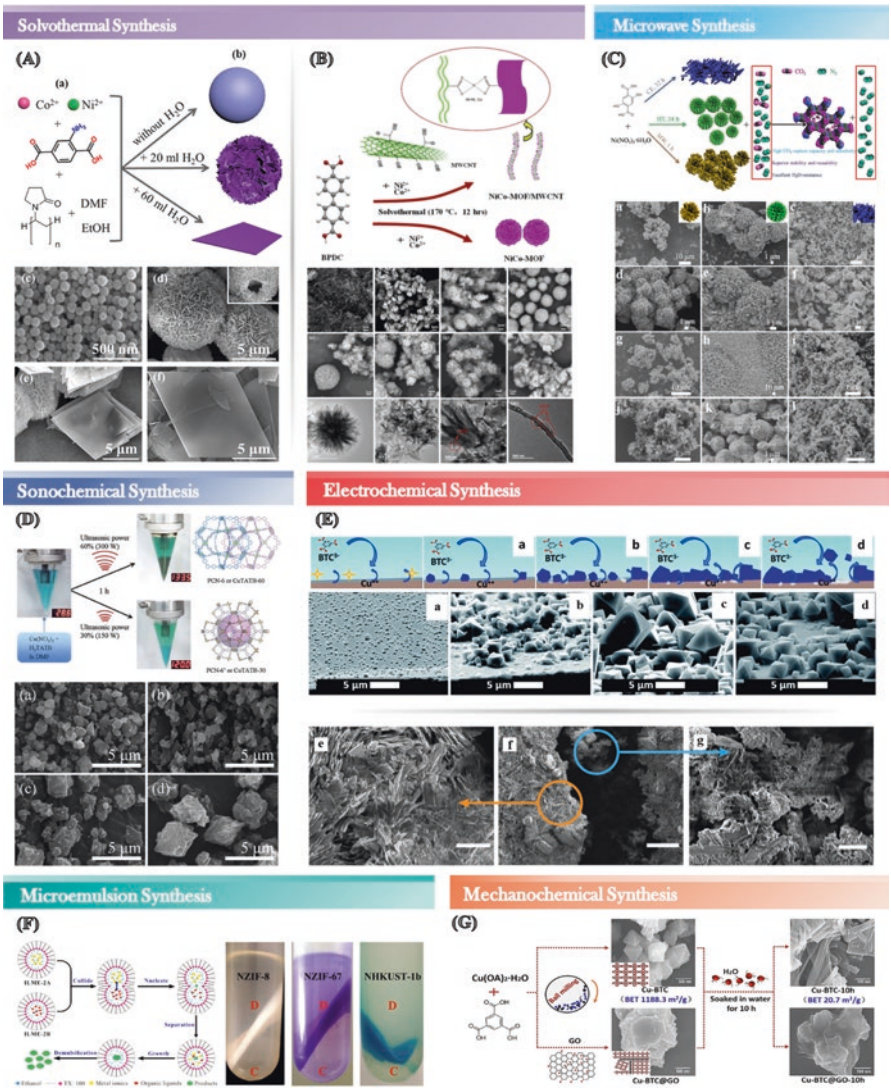

Fig. 8.3 (**A**) Schematic illustration of solvothermal synthesis of NiCo MOF nanostructures with different morphologies (a, b) and SEM images of (c) NiCo-MOF nanosheets (NSs), (d) nanosheet-assembled hollow spheres (NSHS), (e) mixed NSHS and rhombus sheets (RSs), and (f) RSs (*Reprinted with permission from* Sun et al. (2020)), (**B**) SEM and TEM images of carboxylated MWCNTs (a), NiCo-MOF nanostructures (d, j), and NiCo-MOF@MWCNTs particles (b, c, e–h, k–m) (*Reprinted with permission from* Wang et al. (2019a)), (**C**) SEM images of MOF-74 (Ni) nanostructures prepared by MW at (a, d) 125 and (g, j) 140 °C for 60 min, by hydrothermal at (b, e) 125 and (h, k) 140 °C for 24 h and by condensation reflux at (c, f) 125 and (i, l) 140 °C for 32 h (*Reprinted with permission from* Chen et al. (2019a)), (**D**) SEM micrographs of CuTATB nanostructures synthesized sonochemically under different ultrasonic power levels; (a) 30%, (b) 40%, (c) 50%, and (d) 60% (*Reprinted with permission from* Kim et al. (2011)), (**E**) SEM pictures of four phases involved in the anodic electrodeposition of HKUST-1: (I) initial nucleation (a), (II)

(continued)

growth of islands (b), (III) intergrowth (c), and (III) detachment (d) (*Reprinted with permission from* Campagnol et al. (2016)) and cathodic electrodeposition of biphasic metal-organic framework thin film produced by sequential growth at −1.10 and −1.50 V (f), displaying the characteristic feather-like morphology of $(Et_3NH)_2Zn_3(BDC)_4$ in the top layer (e, orange arrow) and the small crystallites associated with the Zn/MOF-5 composite in the layer closer to the electrode surface (g, blue arrow) (*Reprinted with permission from* Li and Dincă (2014)), (**F**) Schematic representation of the growth mechanism of HKUST-1 nanoparticles synthesized through ionic liquid microemulsion technique along with the digital images of ternary system after demulsification and centrifugation (*Reprinted with permission from* Zheng et al. (2017)), (**G**) Mechanochemical synthesis of Cu-BTC and Cu-BTC@GO nanostructures which depicts the BET and water stability of each sample (*Reprinted with permission from* Li et al. (2016b))

8.2.3 Microwave-Assisted Synthesis

Although the solvothermal method comes up with numerous advantages as mentioned in the last section, it is considered as an energy-intensive approach since it requires high temperatures and pressures for a long period of time. To overcome this issue, microwave-assisted synthesis has been proposed as a mechanism of rate enhancement through accelerating the rate of reactions (Meek et al., 2011). In the MW synthesis, a mixture of reactants is transferred to a sealed MW tube and placed in a MW reactor as schematically shown in Fig. 8.2b. Once the reaction vessel is exposed to the MW irradiation, the permanent dipole moment of the molecules or ions in polar solvents can be coupled with the oscillating electric field. Hence, by applying an appropriate frequency, the molecules in the synthesis medium collide which leads to an increase in the temperature of the system. The rapid heating of the solution reduces the reaction time to a great extent (from several days in the solvothermal technique to several minutes for MW method). Moreover, since the rise in the temperature occurs as a result of direct interaction between the electromagnetic waves and electric charges of molecules, homogeneous heating throughout the whole medium is possible which in turn accelerates the crystallization and improves the product purity (Stock & Biswas, 2012). MIL-100(Cr) was the first nanoporous MOF synthesized through the MW route in 2005 (Jhung et al., 2005). The XRD pattern of the as-synthesized chromium trimesate revealed that the particles prepared under MW irradiation at 220 °C for 4 h are comparable in crystallinity with those of synthesized by solvothermal technique at 220 °C for 4 days. So far, numerous MOF nanostructures have been synthesized by means of MW method including MIL-101(Fe) (Taylor-Pashow et al., 2009), Co-MOF-74 (Cho et al., 2012), MOF-205 (Babu et al., 2016), and MOF-74(Ni) (Chen et al., 2019a).

To elucidate the mechanism of the rate enhancement induced by MW conditions, a systematic study was conducted by Jhung group on different MOFs prepared by MW method, and the results were compared with other synthetic routes such as conventional electric heating and solvothermal (Khan et al., 2010; Haque et al., 2010). Their investigations indicated that the mechanism of rate acceleration strongly depends on the type of MOF and can be due to the enhancement in the kinetics of either the nucleation step or the crystal growth. For instance, in the case of HKUST-1 (Cu-BTC MOF), even though both stages are enhanced, the observed

acceleration is mainly due to the nucleation step (Khan et al., 2010). This is while for iron terephthalate (MIL-53(Fe)), the enhancement in the crystal growth plays a more critical role (Haque et al., 2010). It is noteworthy to mention that to obtain high crystalline MOFs with narrow size distribution and desired morphologies, it is essential to control the reaction parameters. Increasing the reaction parameters such as MW irradiation time, power level, and concentration of substrates beyond an optimal condition would result in reduction of the synthesis time at the expense of products' crystallinity. As an example, the results of a study performed on MW-assisted synthesis of MOF-5 showed that prolonging the microwave irradiation time led to a sharp deterioration in its physicochemical properties (Choi et al., 2008). In a recent article published by Chen and coworkers, the effect of synthesis conditions (i.e., hydrothermal (HT), microwave-assisted (MW), and condensation reflux (CE)) on the morphology and physicochemical properties of a series of MOF-74(Ni) was thoroughly investigated (Chen et al., 2019a). It was shown that the MW method is a facile and rapid (within 60 min) approach for preparing MOF-74(Ni) particles compared to those of HT (24 h) and CE (32 h) techniques. Furthermore, the materials prepared via MW route demonstrated smaller and relatively more uniform particle size as well as higher thermal stability as depicted in Fig. 8.3c.

8.2.4 Sonochemical Synthesis

Sonochemical synthesis refers to the use of high-energy ultrasound to a liquid that generates bubbles in the reaction mixture in which ultrasonic energy is accumulated. The formed bubbles start to grow gradually and, once reaching a certain size, collapse instantaneously. The process of formation, growth, and implosive collapse of the microbubbles in the medium is called "acoustic cavitation." This phenomenon results in the formation of localized "hot spots" with extremely high temperatures (~5000 K) and pressures (~1000 bar) throughout the solution (Suslick et al., 1986). Hence, free radicals are formed through the remarkable increase in the reaction conditions (i.e., temperature and pressure), and as a consequence, homogeneous nucleation centers are generated (Al Amery et al., 2020). As a result, a sonochemical method can be applied to produce small MOF nanocrystals with higher degree of crystallinity within considerably shorter reaction times (compared to conventional solvothermal technique). Various experimental conditions such as type of solvents, concentration of the substrates, pH of solution, the applied ultrasound power, as well as reaction time and duration of ultrasonication should be considered to achieve MOFs with desired structures (Cho et al., 2013; Abdollahi et al., 2018; Armstrong et al., 2017; Kim et al., 2011). Different equipment with adjustable power outputs including reactors equipped with high-power ultrasonic horns (Fig. 8.2c) or ultrasonic baths (with relatively lower power intensities) can be utilized in this regard. The choice of the instrument used is important since the ultrasound frequency and intensity has a direct influence on the crystallization. For instance, CuTATB-n where TATB is 4,4′,4″-s-triazine-2,4,6-triyltribenzoate and n

represents the power level were synthesized in 1 h by adjusting the ultrasonic power level (Kim et al., 2011). As clearly shown in the SEM images of Fig. 8.3d, by increasing the power level from 30% to 60%, a progressive increase was observed in the particle size. After precise characterizations, it was concluded that at 30% ultrasonic power, PCN-6′ was produced, while at 60% power intensity, PCN-6 (the catenated form) with higher surface area and enhanced stability of the network was obtained. In the past few years, as an environmentally friendly method, sonochemical route has been used for synthesizing numerous MOF structures (Cho et al., 2013; Abdollahi et al., 2018; Armstrong et al., 2017; Kim et al., 2011; Son et al., 2008; Jung et al., 2010; Dastbaz et al., 2019) due to its advantages, namely, rapidity, facility, and energy-efficiency which allows the scale up of MOF's production. This is while more investigations are yet needed to be done for better comprehension of the involved mechanism.

8.2.5 Electrochemical Synthesis

Electrochemical method is another promising technique which is suitable for deposition of MOF thin films on the surface of conductive substrates. In electrochemical deposition of MOFs, the substrate of interest is immersed in an electrolyte solution containing organic ligands. Subsequently, by applying appropriate conditions (voltage or current density), a thin layer of MOF is grown on the surface of the substrate. The electrodeposition technique can be performed via two different routes: anodic and cathodic deposition in a two-electrode cell configuration (Al-Kutubi et al., 2015; Campagnol et al., 2016; Li et al., 2016a).

In anodic deposition, the metal ions are electrochemically produced through anodic dissolution of anode material which then react with the deprotonated organic ligands in the electrolyte solution. The result is the formation of a thin MOF layer on the surface of anode as schematically shown in Fig. 8.2D-a. Since the metallic electrodes (such as Cu and Zn) are utilized in anodic deposition as the source of metal ions, the use of metal salts is avoided during the synthesis which in turn eliminates the formation of hazards associated with anions such as nitrates, perchlorate, or chloride (Stock & Biswas, 2012; Lee et al., 2013; Dey et al., 2014). The first report on electrochemical synthesis of MOFs was published in 2005 by researchers of BASF (Mueller et al., 2007). They made use of copper plates as both cathode and anode electrodes in a methanol electrolyte containing H_3BTC as the organic ligand. By applying a voltage of 12–19 V for a duration of 150 min followed by an activation step, copper (II) trimesate framework of HKUST-1 was prepared through anodic deposition. From then on, their pioneering work was further extended to synthesis various metal-organic frameworks such as ZIF-8, MIL-100 (Al), MIL-53 (Al), and NH_2-MIL-53 (Al) via anodic electrodeposition (Martinez Joaristi et al., 2012; Hauser et al., 2019; Stassen et al., 2015).

Another approach for the formation of MOF thin film is based on providing the metal centers from an electrolyte solution containing metal salts rather than metallic

oxidation. The metal ions present in the solution coordinate with the deprotonated organic ligands near the cathodic electrode which are generated either by OH^- ions produced through reduction of water at the surface of cathode or anions such as NO_3^- from the nitrate salts. In the other words, the increase in the pH of the electrolyte solution near the cathodic electrode surface as a result of OH^- ions formation led to the deprotonation of neutral organic linkers which then react with the metal ions and subsequent deposition of MOF layer on the surface of cathode. This approach which is known as "cathodic deposition" (Fig. 8.2D-b) was adopted to synthesis MOF nanostructures on the electrode surface (Li & Dincă, 2014; Zhu et al., 2015; Wei et al., 2020; Xiao et al., 2020). Figure 8.3E depicts the scanning electron micrographs of MOF layers grown on the surface of electrodes via anodic and cathodic deposition (Campagnol et al., 2016; Li & Dincă, 2014). In order to obtain an adherent microporous layer of MOF with textural properties, the effect of synthesis parameters including type of the solvent, type and concentration of the electrolyte, the applied voltage or current-density, and temperature and duration of the electrodeposition should be precisely controlled.

Electrochemical deposition method has several advantages including the possibility of synthesizing thin films of metal-organic frameworks under mild preparation conditions (compared to solvothermal technique, it operates at relatively low temperatures within a short period of time). In addition, it is of great interest for direct growth of MOF layers on a conductive substrate. Moreover, by altering the reaction parameters (i.e., voltages and current density) along with the deposition time, it is possible to tune the thickness of deposited MOF coatings with controlled phase and morphology. All these properties together turn electrochemical synthesis into an appropriate approach for large-scale production processes. However, the mechanisms of growth should be yet investigated to achieve a deeper insight for further design and preparation of MOF nanostructures.

8.2.6 Microemulsion Synthesis

Microemulsions are thermodynamically stable dispersions of water and oil mixtures in the presence of surfactants molecules. When a surfactant is added to an immiscible water/oil mixture, small droplets (size <100 nm) are formed spontaneously due to the self-assembly of these amphiphilic molecules in which the dispersed phase is retained. There are three main types of microemulsions including "direct" as for oil dispersed in water, "reversed" which refer to dispersed water in a continuous organic phase, and "bicontinuous." These droplets can act as nanocontainers inside which the dissolved starting materials react together within a confined area. From this perspective, microemulsion synthesis approach is of great value for preparing nanoparticles with small size and narrow size distribution (Flügel et al., 2012). Various approaches have been adopted for the formation of microemulsion in order to synthesis nanoMOFs (Sun et al., 2016; Zheng et al., 2017; Shang et al., 2013; Ye et al., 2018). For instance, ZIF nanocrystals were synthesized through

reverse microemulsion technique as well as ionic liquid microemulsion (Sun et al., 2016; Zheng et al., 2017). In reverse microemulsion, as schematically shown in Fig. 8.2F, the precursors are dissolved separately in appropriate solvents, and then, the solutions are mixed together to form a stable water in oil dispersion. As an example, Sun et al. synthesized monodispersed ZIF nanostructures (ZIF-8 and ZIF-67) with extremely small size (<5 nm) at room temperature and through reverse microemulsion (Sun et al., 2016). Their synthetic route is based on the addition of solutions containing the starting materials (i.e., $Zn(NO_3)_2{\cdot}6H_2O$ in water as solution I and 2-MIm/triethylamine in water as solution II) to the CTAB/1-haexanol/heptane mixture. The prepared ZIF nanoparticles showed high surface area and thermal stability. On the other hand, Zheng and coworkers synthesized nanoscale ZIFs by the ionic liquid-containing microemulsion system of H_2O/BmimPF$_6$/TX-100 (Zheng et al., 2017). As depicted in Fig. 8.3F, HKUST-1 nanoparticles could be also synthesized by adding ethanol into the H_2O/TX-100/BmimPF$_6$ system in order to improve the dissolution of organic ligands. These examples demonstrate that by careful adjustment of the reaction composition, different MOFs with controlled shape and morphology are achievable.

8.2.7 Layer-by-Layer Growth

The layer-by-layer (LBL) growth is an approach composed of immersing a substrate in the solutions of metal salt and organic linker, respectively. After each immersion step, a molecular layer is formed on the surface (Fig. 8.2G). As its name implies, a homogeneous nanoscale film of MOF can be grown by successive deposition steps. The thickness of MOF layer can be controlled through the number of repeated cycles of immersion in the solutions of precursors, while its crystal direction is tunable via using modified substrates with special functional groups (Shekhah et al., 2007; Zacher et al., 2009; Shekhah, 2010; Yuan & Zhu, 2020).

The step-by-step route was developed for the growth of various MOF thin films (Shekhah et al., 2009; So et al., 2013; Li et al., 2014). Shekhah et al. reported on the formation of a highly ordered and oriented HKUST-1 layer on the surface of gold substrate (Shekhah et al., 2009). To this end, well-defined organic surfaces were prepared by fabricating self-assembled monolayers (SAMs), namely, COOH- and OH-terminated SAMs, on the surface of Au substrates as the growth templates. It was found that the growth direction strongly depends on the type of functional groups since for COOH-functionalized surface, the growth of [Cu_3-(btc)$_2$] proceeded along the (Shang et al., 2013) direction, while an OH-terminated surface favors the formation of a MOF layer with (Biswal et al., 2013) orientation. Compared to direct growth method, the layer-by-layer approach allows for obtaining homogeneous films with preferred orientation at mild conditions (i.e., room temperature). However, it can be classified as a time-consuming process since it needs pre-functionalized substrates with SAMs as well as immersion/washing repetitive cycles to obtain MOF layers with a certain thickness.

8.2.8 Mechanochemical Synthesis

Mechanochemistry refers to the chemical reactions which are induced by mechanical forces that break the intramolecular bonds. Unlike all the abovementioned methods which rely on solvents, mechanochemical synthesis is a solid-state reaction which means that it is a solvent-free technique. As schematically represented in Fig. 8.2E, in the mechanochemical method, the precursors (i.e., metal salts and organic ligands) are mixed together and then ground in a ball mill grinder. Pichon et al. were the first to report solvent-free synthesis of a microporous $[Cu(INA)_2]$ metal-organic framework by grinding $Cu(OAc)_2{\cdot}3H_2O$ and isonicotinic acid (INA) (Pichon et al., 2006). From then on, various MOFs have been synthesized through mechanochemical methods (Klimakow et al., 2010; Biswal et al., 2013; Li et al., 2016b; Chen et al., 2019b; Wang et al., 2020). This technique can be used not only to synthesize pure MOF crystals but also to prepare MOF hybrid structures. For instance, Cu-BTC@GO composites were mechanochemically synthesized within 30 min (Li et al., 2016b). As shown in the SEM images of Fig. 8.3G, the water stability of Cu-BTC framework was remarkably enhanced after compositing with graphene oxide nanosheets.

In order to increase the reactivity of mechanochemical synthesis, organic reactants with low melting point along with hydrated metal salts (such as metal acetates or carbonates) are preferred. The mechanochemical is advantageous for synthesizing MOF structures from different perspectives: it is an environmentally friendly approach compared to liquid-phase reactions, because the organic solvents are avoided in such a solvent-free technique. Moreover, porous MOF nanocrystals can be obtained at room temperatures within short reaction times with quantitative yields which makes it appropriate for scaling up.

8.3 Biomedical Applications of MOF Nanoparticles

Recent years have witnessed a dynamic development in early diagnosis and treatment of diseases. The emergence of nanotechnology has undoubtedly played a pivotal role in this regard and opened up new horizons in various fields of nanomedicine specially for early detection and targeted therapy of cancers. As mentioned previously, cancer treatment strongly depends on detection of the disease at primary stages followed by localized therapy in such a way that healthy tissues and organs are not affected. With the intense evolution of imaging modalities, nanoparticle probes have been utilized for molecular imaging to assist with the cancer diagnosis. Typical contrast agents such as iodine, barium, and gadolinium, although providing valuable information, are associated with certain drawbacks including nonspecific biodistribution, short blood half-life, fast clearance from the body, and slight renal toxicity (Naseri et al., 2018). Therefore, developing targeted contrast agents with high sensitivity and specificity for noninvasive diagnosis purposes is of tremendous

importance. Nanoparticles represent a promising strategy for biomedical imaging which encompass prolonged circulation half-lives and higher in vitro and/or in vivo stabilities.

Moreover, nanoscale cargo delivery systems which can be used to deliver drugs, nucleic acids, ligands, or antibodies show great potential in cancer treatment (Mi et al., 2020). Compared to conventional cancer therapies such as chemotherapy and radiotherapy which suffer from nonspecific biodistribution and targeting as well as poor oral bioavailabilities, cancer nanotherapeutics make use of nanoparticles not only to improve pharmacokinetics and biodistribution but also to increase the blood circulation time. Moreover, nanoparticles are beneficial for increased concentration in the target site by passive accumulation at the tumor microenvironments due to the enhanced permeability and retention (EPR) effect. These properties reduce the toxicity and side effects and, as a result, enhance their therapeutic efficiency (Shi et al., 2017).

Among various kinds of nanostructures, MOFs have attracted considerable attention for nanomedical applications because of their unique characteristics such as tunable pore size and structure, large surface areas, biodegradability, and functionalization versatility. In one hand, their high specific surface area allows for functionalization with various small molecules such as drugs and therapeutic agents, while on the other hand, the wise selection of metal ions (like those of paramagnetic or superparamagnetic) and organic ligands (such as luminescent ones) makes them prone for imaging applications. These features have led to the emergence of MOF-based theranostic nanoplatforms which enable the integration of both diagnostic and therapeutic functions at the same time and in one entity (Cai et al., 2015). In addition to the advantages of nanoMOFs (nMOFs) for drug delivery and imaging applications, incorporating extra materials into a MOF structure or preparing MOF composites can also enhance the efficacy of MOF systems in biomedical applications (Osterrieth & Fairen-Jimenez, 2020). In the following sub-sections, we first enumerate the applications of MOFs for biomedical imaging as well as for drug delivery purposes. Then, various MOF-based nanostructures with potential for theranostic goals will be discussed.

8.3.1 Biomedical Imaging

Nanoparticles are proved to be promising candidates for biomedical imaging due to their capabilities in producing signals or even enhancing the signal contrast at tumor sites. In the realm of bioimaging, nanoMOFs offer numerous advantages as contrast agents which relates to the fact that their composition and structure and, as a result, their physicochemical properties can be tuned by reasonable choice of metal ions/clusters as well as organic linkers (Yang & Yang, 2020; Li et al., 2019a). For this reason, nMOFs have been exploited as powerful diagnostic tools for magnetic resonance imaging (MRI), X-ray computed tomography (CT), positron emission tomography (PET), and photoacoustic (PA) and optical imaging techniques (Deng et al.,

2017; Yang et al., 2019; Robison et al., 2019; Peller et al., 2018; Taylor et al., 2008; Horcajada et al., 2010; Pereira et al., 2010; Tian et al., 2015; Chen et al., 2017; Shang et al., 2017; Zhang et al., 2018a).

In 2017, Deng et al. designed a fluorescent probe composed of encapsulated Rhodamine B (RhB) into nanoscale ZIF-90 particles for mitochondrial ATP sensing and imaging in living cells (Deng et al., 2017). The competitive coordination between ATP molecules and the metal centers of ZIF-90 decomposes the zeolitic framework structure and, as a consequence, releases the RhB. It was argued that through this ATP-triggered release mechanism, monitoring of ATP molecules which are mainly produced in mitochondria is possible which is of value to study the process of cellular respiration and disease diagnosis. A two-photon Zr-based MOF (PCN-58) was also applied as a sensing platform for intracellular sensing and deep tissue imaging (Yang et al., 2019). The incorporation of a target-responsive two-photon organic moiety into the MOF structure through click chemistry resulted in a fluorescent probe with high signal-to-noise ratio, photostability, and deep tissue penetration. The structure was designed in such a way that ensures large enough cavities for loading fluorophores. As schematically shown in Fig. 8.4A (a and b), PCN-58 was covalently cross-linked with two-photon fluorescent organic probes via Cu(I)-catalyzed azide-alkyne cycloaddition (CuAAC) without any cross-reactivity toward the MOF structure or other functional groups. The synthesized probe retained its fluorescence-responsive properties corresponding to the two-photon organic moiety with a penetration depth up to 130 μm (Fig. 8.4A-c and d).

X-ray computed tomography (CT) is another common diagnostic method used in the medical field. A new cluster-based bismuth metal-organic framework (Bi-NU-901) which consists of eight connected Bi_6 nodes and tetratopic pyrene-based linkers was synthesized solvothermally and tested as a CT contrast agent (Robison et al., 2019). The results revealed that the prepared Bi-MOF with robust chemical and thermal stability demonstrated ∼7 times better contrast intensity compared to the zirconium analogue (Zr-NU-901) and ∼14 times superior than that of a commercially available CT contrast agent (idixanol).

In addition, metal-organic frameworks have also paved their way toward magnetic resonance imaging as one of the most versatile imaging modalities being used in routine clinical examinations that provides high spatial resolution images (Peller et al., 2018). Regarding the contrast agents used in MRI such as gadolinium, the safety issue is a major concern since Gd ions can leak from the chelate complex during their application. In this respect, three different approaches have been adopted to construct MRI active MOF nanoparticles (Peller et al., 2018). In the first concept, the metallic centers are responsible for MRI contrast such as in Gd-, Mn-, and Fe-based MOFs (Taylor et al., 2008; Horcajada et al., 2010; Pereira et al., 2010; Tian et al., 2015). The high chemical stability of MOF complexes minimizes the metal leakage to a great extent and leads to biocompatibility issues. The second concept is based on growing a MOF shell on the surface of MRI-active metal oxide nanoparticles, while in the third strategy, post-synthetic modification procedures are used to functionalize the external surface of MOFs with contrast agents (Peller et al., 2018). The latter two cases are generally utilized for theranostic applications

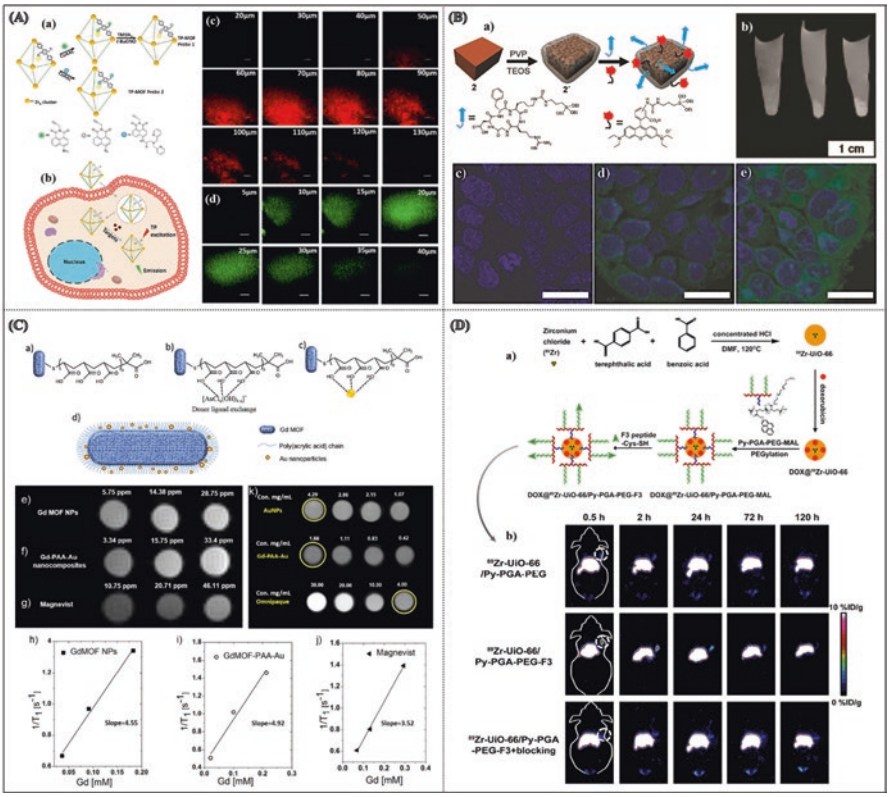

Fig. 8.4 Examples of nMOFs for various biomedical imaging applications; (**A**) Schematic illustration for the preparation of two photon (TP)-MOF sensing platform and the process of intracellular sensing (a, b); Depth fluorescence images of TP-MOF probe 1 in rat liver tissue in which the change of FL intensity with scan depth was determined by spectral confocal multiphoton microscopy (c) or one-photon microscopy (d) in the z-scan mode (the scale bar is 50 μm) (*Reprinted with permission from* Yang et al. (2019)); (**B**) Mn-based MOF nanoparticles synthesized via MW method were coated with a thin silica shell (denoted as 2′) in order to stabilize them as well as facilitating their functionalization with a fluorophore and c(RGDfK) cell-targeting peptide (a), In vitro MR images of HT-29 cells incubated with 2′ (left), nontargeted 2′ (middle) and c(RGDfK)-targeted 2′ (right) (b), Merged confocal images of HT-29 cells that were incubated with 2′ (c), nontargeted 2′ (d) and c(RGDfK)-targeted 2′ (e); The blue color was from DRAQ5 used to stain the cell nuclei while the green color was from RhB. The bars represent 20 μm (*Reprinted with permission from* Taylor et al. (2008)), (**C**) Schematic representation of the Gd-MOF/PAA/Au nanocomposite preparation (a-d), T_1-weighted MRI images and relaxation rate ($1/T_1$) as a function of the Gd concentration for unmodified Gd-MOF nanoparticles (e, h), Gd-MOF/PAA/Au nanocomposite (f, i), and chelate-based Gd contrast agent (Magnevist) (g, j) at various Gd concentrations in DIUF water, CT images of plain AuNPs, Gd-MOF/PAA/Au nanocomposite, and the iodine-based contrast agent Omnipaque with different Au or iodine concentration (k) (*Reprinted with permission from* Tian et al. (2015)), (**D**) Schematic synthesis route of ^{89}Zr-UiO-66/Py-PGA-PEG-F3 conjugates (a) and representative coronal PET images of MDA-MB-231 tumor bearing mice at different time points post-injection for various nanostructures with excessive amount of F3 peptide blocking; The location of tumors was identified by dashed circles (b) (*Reprinted with permission from* Chen et al. (2017))

as they can merge the advantages of potentially MRI active agents for imaging purposes with extremely high porosity of MOFs as drug carriers for therapeutic goals. Mn-containing nMOFs with various morphologies were synthesized through reverse-phase microemulsion method at room temperature and MW-assisted synthesis at 120 °C (Taylor et al., 2008). The as-prepared particles demonstrated very high in vitro and in vivo longitudinal relaxivity (r_1) with excellent MR contrast enhancement. The surface of MW-synthesized MOF nanoparticles was further modified with a thin silica shell which made it possible to covalently attach a cyclic RGD peptide (c(RGDfK)) and an organic fluorophore, as schematically depicted in Fig. 8.4B-a. In one hand, the cell-targeting molecules (c(RGDfK)) enhanced the delivery of the prepared core-shell hybrid nanostructures to the cancer cells, while on the other hand, the silica shell provided an adequate protection until reaching the tumor site where Mn^{2+} ions are released to give T_1-weighted contrast enhancement (Fig. 8.4B, b-e). Nontoxic iron-based MOFs (MIL-88A) were also used as contrast agents for MR imaging (Horcajada et al., 2010). As raised by the authors, the efficiency of the prepared MIL nMOFs in MRI is directly related to their relaxivity by modifying the relaxation times of the water protons in the surrounding medium in the presence of a magnetic field, since MIL nanoparticles not only possess paramagnetic iron atoms in their matrix but also offer an interconnected porous network filled with metal coordinated and/or free water molecules. MOFs containing Ln^{3+} ions with high transverse relaxivity (r_2) were also reported as potential MRI contrast agents for T_2-weighted imaging (Pereira et al., 2010). Gd is one of the most used rare earth elements in MRI medical diagnosis due to its seven unpaired electrons and a large magnetic moment. Tian et al. proposed the Gd MOF nanoparticles synthesized through microemulsion process as an efficient MRI contrast agent (Tian et al., 2015). In the next step and in order to achieve MRI/CT bimodal imaging, Gd MOF nanoparticles were covered with a thin polymeric layer of poly (acrylic acid) (PAA) via reversible addition-fragmentation chain transfer (RAFT) polymerization which is used as a linker between Gd MOF and Au nanoparticles. Finally, Au nanoparticles were deposited on the surface to obtain Gd MOF-PAA-Au nanocomposites, as schematically shown in Fig. 8.4C (a-d). Hence, the prepared nanocomposite can be also exploited as a CT imaging agent. The T_1-weighted MR images as well as relaxation rate ($1/T_1$) studies (Fig. 8.4C, e-j) demonstrated that even at lower concentration, Gd MOF nanoparticles offered brighter images compared to the clinically used chelate-based Gd contrast agent (i.e., Magnevist) and its performance was not hindered by the surface modification procedure. Moreover, the results of CT were also compared to that of clinically used iodine-based contrast agent (Omnipaque), and the results showed higher X-ray attenuation for Gd-PAA-Au nanocomposites than Omnipaque with similar concentrations (Fig. 8.4C-k).

Positron emission tomography (PET) scan is another functional imaging technique with superior detection sensitivity (down to picomolar range) that utilizes radioactive substances (radiotracers) to visualize the biomedical functions of tissues. MOFs with intrinsically radioactive metal nodes can be used for PET imaging. For instance, UiO-66 nMOF (^{89}ZrUiO-66) composed of positron-emitting isotope zirconium-89 (^{89}Zr) was synthesized by a solvothermal method (Chen et al., 2017).

The prepared MOF nanoparticles were loaded with doxorubicin (DOX) with high payload followed by further functionalization with pyrene-derived polyethylene glycol (Py-PGA-PEG) and conjugation with a peptide ligand (F3) to nucleolin for targeting of triple-negative breast tumors (Fig. 8.4D-a). The ability of functionalized UiO-66 conjugates was investigated for PET-guided cargo delivery to cancerous sites. Figure 8.4D-b depicts the representative coronal PET images of MDA-MB-231 tumor-bearing mice regarding the distribution/clearance profile at different time points post-injection for various UiO-66 structures. The results revealed that ^{89}Zr-UiO-66/Py−PGA-PEG-F3 can serve as a potential image-guidable, tumor-selective cargo delivery nanoplatform.

It is noteworthy to mention that in some certain cases, single-modality imaging cannot provide sufficient features on its own. Moreover, each of the previously mentioned techniques is associated with some inherent defects such as low tissue penetration rate, poor special resolution, and low sensitivity. Therefore, multimodal imaging techniques have been proposed to overcome these issues over the past few years. Various MOF nanoarchitectures were used for this purpose by integrating materials with different functionalities (Cai et al., 2017; Shang et al., 2017; Zhang et al., 2018a). For instance, core-shell Au@MIL-88(Fe) nanoparticles were prepared through a microemulsion method and further used for multimodality imaging-based glioma diagnosis (Shang et al., 2017). The potential of the as-prepared Au@MIL-88(Fe) nanocomposites as a triple-modality CT/MR/PA-imaging contrast agent was investigated using a U87 MG-subcutaneous tumor-bearing mice. The CT, T_2-weighted MR, and in vivo PA images of mice before and after intravenous injection as well as the bioluminescent image of tumor demonstrate a remarkable enhancement after injection with the nanocomposite. The results represent that Au@MIL-88(Fe) nanoparticles with low cytotoxicity provide a contrast agent with substantial enhancement of imaging sensitivity, high depth of penetration, and spatial resolution for imaging of glioma. Other multimodal imaging such as FL/PA/T_2-weighted MR imaging based on hyaluronic acid and ICG-engineered MIL-100(Fe) NPs (Cai et al., 2017) or doxorubicin (DOX)@Gd MOFs-glucose nanocarrier for CT/T_1-weighted MR imaging (Zhang et al., 2018a) were also reported.

8.3.2 MOF-Based Therapeutic Systems

The development of controllable drug delivery systems (DDSs) capable of transporting therapeutic agents as well as their subsequent release in a targeted manner (without reaching the nontarget cells, organs, or tissues) is indispensable to reduce the side effects and enhance the therapeutic efficacy of drugs (Sousa et al., 2019; Mir et al., 2017). In the meantime, phototherapy techniques including photodynamic therapy (PDT) and photothermal therapy (PTT) have attracted a great deal of attention for treating cancer due to their minimally invasive nature and minor collateral damages to the surrounding normal tissues (Dolmans et al., 2003; Doughty et al., 2019). In PDT, photoactive molecules called photosensitizer (PS) generate

reactive oxygen species (ROS) through a series of photochemical reactions upon absorbing light with a specific wavelength which will consequently lead to cell death. Photothermal therapy refers to the use of photothermal agents which can convert light (most often in infrared wavelengths) to heat energy for local hyperthermia and tumor treatment. When a photosensitizer is stimulated by an electromagnetic radiation, it can absorb energy through excitation and then release the vibrational energy (heat). This photon-mediated process results in elevating the local temperature to 41–47 °C which ultimately can kill the targeted cells.

Conventional carriers such as liposomes, micelles, or nanoparticles are commonly associated with low drug capacity and, as a result, poor loading. This is while nMOFs hold great promise for drug storage and delivery considering their highly porous topology along with the possibility of designing these structures with suitable biocompatibility (Sun et al., 2013; Wang et al., 2018a; Cao et al., 2020). Moreover, their structural robustness prevents undesirable decomposition and burst release.

There exist three different approaches for loading the drug molecules on nMOFs based on the location of the drug as well as the host-guest interactions (Fig. 8.5A) (Wang et al., 2018a). In the first approach, drug molecules are encapsulated in the void volume (channels, pores, and cavities) of porous nMOFs (Fig. 8.5A-a). To this end, MOF nanoparticles are first synthesized through an appropriate method and then exploited for loading of drugs via either covalent or noncovalent interactions. The efficiency of encapsulation strategy strongly depends on the size of therapeutic substances compared to the pore size and structure of MOF carriers and should be carefully adjusted to obtain high loading capacities. Direct assembly is another method for incorporation of drug molecules into MOF structures. As shown in Fig. 8.5A-b, in the direct assembly method, the drug molecules or their prodrug formulations with suitable functional groups are used as linkers between metallic centers through coordination bonds. Under physiological conditions, the MOF nanoparticles are decomposed slowly which in turn release the active therapeutic components. Compared to the encapsulation technique, direct assembly is of advantage since inserting the drug molecule as a ligand into the structure results in more uniform distribution with higher loadings. However, controlling the reaction parameters in order to achieve the expected MOF structures is more challenging. The direct assembly approach has been successfully used for incorporation of some chemotherapeutic drugs such as methotrexate (MTX) (Huxford et al., 2012), bisphosphonates like pamidronate (Pam) (Liu et al., 2012), and cisplatin and oxaliplatin prodrugs (Liu et al., 2014a; Rieter et al., 2008) into MOF matrix. The third strategy for drug loading proceeds via a post-synthetic modification in which the guest molecules are covalently attached to a pre-synthesized MOF through formation of coordination bonds with metal centers or covalent bonds with the functional sites of the organic linkers (Fig. 8.5A-c) (Wang et al., 2018a).

Furthermore, the application of nanoscale MOFs in phototherapy, as a clinically approved technique for treatment of cancer, has been also investigated (Guan et al., 2018; Lan et al., 2019; Boddula et al., 2020; Hu et al., 2018; Wang et al., 2018b, 2019b; Li et al., 2019b; Li et al., 2020). The characteristic features of these porous

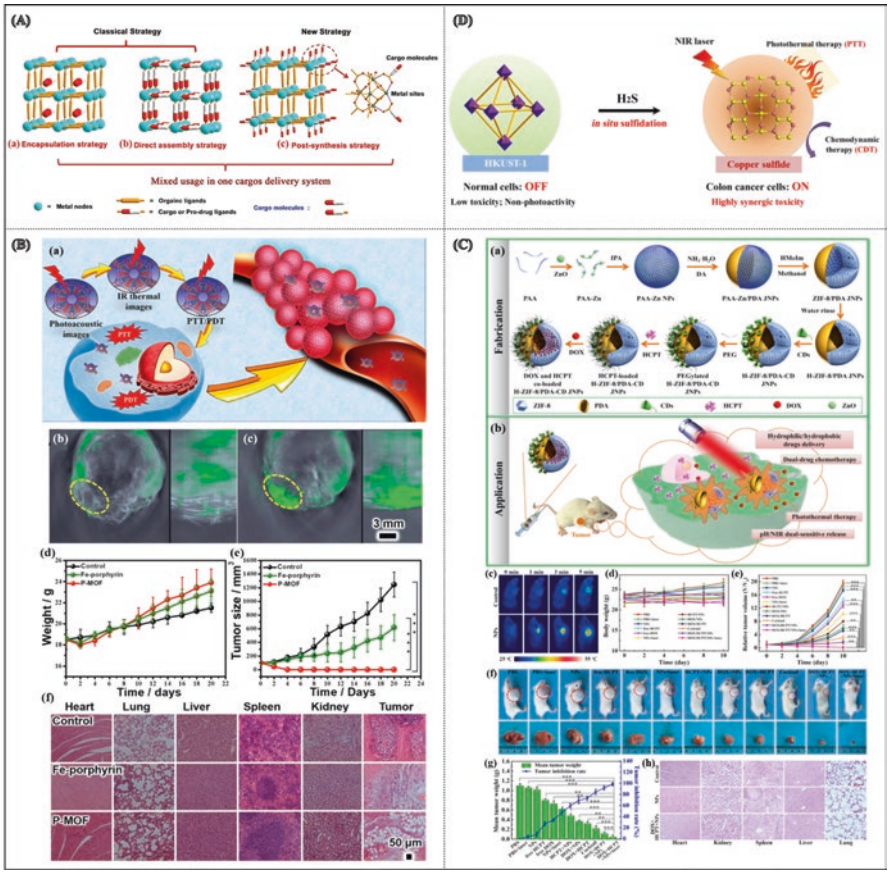

Fig. 8.5 Therapeutic applications of nMOFs; (**A**) Three different cargo-loading strategies for MOFs: "Encapsulation" in which drug molecules are entered into the pores or channels of MOF and maintained via noncovalent interactions (a), "Direct assembly" which uses drug/prodrug molecules as ligands to partly participate in the formation of MOFs via coordination bonds (b) and "Post-synthesis" that comprises the formation of coordination bonds between cargo molecules and unsaturated metal sites or ligand defect sites of pre-synthesized MOF structures (*Reprinted with permission from* Wang et al. (2018a)), (**B**) Schematic representation of PDT/PTT cancer cotherapy as well as PA imaging based on NIR-stimulation of single atom iron centers in PMOF (a), 3D multispectral photoacoustic tomography (MSOT) image and enlarged orthogonal views of tumor after the injection of PBS (b), PMOF under 808 nm laser irradiation (c), Body weights of various mice groups after the therapy (d), Tumor growth curves under different treatments (Statistical analysis, $^{***}p < 0.001$), (e) and H&E-stained main organs and tumor slices obtained from different groups of mice following different therapies (f) (*Reprinted with permission from* Wang et al. (2019b)), (**C**) Fabrication process of H-ZIF-8/PDA-CD JNPs used in dual-drug chemotherapy and photothermal therapy (a, b), IR thermal images of tumor-bearing mice administrated with PBS and H-ZIF-8/PDA-CD JNPs under 808 nm laser irradiation (c), The body weight of mice (d), Tumor growth curves of mice (e), Digital images of mice and excised tumors in the groups with various treatments (f), The mean tumor weight and the tumor inhibition rate of each group on the last day of experiments (g), and H&E stained histological sections of major organs (Statistical significance: $^{**}p < 0.01$, $^{***}p < 0.001$) (h) (*Reprinted with permission from* Li et al. (2019b)), (**D**) Schematic of the H_2S-triggered transformation of non-photoactive HKUST-1 nanoenzyme into an NIR-activatable photothermal agent by in situ sulfidation reaction used for synergic photothermal and chemodynamic therapy for colon cancer (*Reprinted with permission from* Li et al. (2020))

crystalline materials turn them into potential candidates for photo-induced therapeutic purposes. MOFs can be either used as photosensitizers themselves or exploited as a carrier for exogenous photosensitizers due to their porous structure with high specific surface area. Since PSs have low water solubility and tend to aggregate easily as a result of their organic nature with high degree of conjugation, the encapsulation strategy assists in increasing their solubility, hence improving their cellular uptake. Last but not least, these nanoplatforms can be used for phototherapies in combination with the loading and release of chemotherapy drugs which will reduce the long-term morbidity (Boddula et al., 2020).

Hu et al. encapsulated different kinds of PSs (i.e., Ce6, TPEDC, and TPETCF) in MIL-100(Fe) as a general inert carrier (Hu et al., 2018). The encapsulation process blocked the photosensitizing capability of the aforementioned compounds as a result of their isolation from oxygen (O_2). After reaching the tumor site with excess H_2O_2 secretion, the framework collapsed and released the encapsulated PSs which led to recovered photosensitization and activated PDT. In addition, it was observed that in comparison to the original PSs, the recovered photosensitization underwent enhanced PDT due to the relieving of hypoxia by O_2 generated from the reaction between Fe (III) and H_2O_2. In another study conducted by Wang and coworkers, a multifunctional MOF-based hybrid nanogel was synthesized through in situ polymerization of dopamine monomers encapsulated in the pores of a MnCo MOF structure ($Mn_3[Co(CN)_6]_2$) and named as MCP nanoparticles (Wang et al., 2018b). Polydopamine (PDA) is found to be a promising PTT agent due to its NIR absorption. The prepared MCP nanoparticles were further modified with polyethylene glycol (PEG) in order to increase the in vivo stability, biocompatibility, and blood circulation time of MCP as well as with thiol terminal cyclic arginine-glycine-aspartic acid peptide to ensure the tumor accumulation of MCP-PEG nanoparticles and improve their therapeutic efficiency as photothermal agent. The resulting hybrid nanostructure could also have served as a positive T_1 MR contrast agent as well due to the high-spin Mn-N_6 ($S = 5/2$) in the skeleton of MnCo. The results revealed that the obtained nanocomposite offers numerous advantages over commonly explored photothermal agents including uniform size distribution, long-term solution stability, enhanced photothermal conversion efficiency, and higher tumor accumulation.

Dual photodynamic and photothermal (PDT/PTT) co-therapy is another way of exploiting the therapeutic potential of nMOFs. For instance, a porphyrin-like single atom Fe(III)-containing MOF (denoted as PMOF) was synthesized and evaluated for PDT/PTT co-therapy under NIR (808 nm) irradiation as well as for PA imaging (Fig. 8.5B-a) (Wang et al., 2019b). The prepared PMOF nanocrystals demonstrated not only excellent performance for modulation of the hypoxic tumor microenvironment of HeLa cell tumors in mice but also good properties as a photoacoustic imaging (PAI) agent which were attributed to the abundant single atom Fe(III) centers (as shown in Fig. 8.5B, b-f). The results of density functional theory (DFT) calculations revealed that this superior performance is related to the narrow HOMO-LUMO band gap energy of 1.31 eV which enabled strong absorption of NIR photons while irradiated and resulted in promoted PTT. Moreover, the presence of porphyrin-like Fe(III) nodes assists in generating singlet oxygen ($^1O_2$) from triplet one ($^3O_2$), hence

benefiting PDT. In another attempt, spherical zeolitic imidazolate framework-8/polydopamine Janus nanoparticles with hollow structure (H-ZIF-8/PDA JNPs) were first prepared through a mild synthesis strategy, and then, PDA chains were further functionalized with β-cyclodextrins (CDs) (Li et al., 2019b). The resultant composite was explored as a multifunctional platform for cancer treatment via synergistic dual-drug chemotherapy and PTT as schematically depicted in Fig. 8.5C-a, b. The obtained results can be attributed to the following characteristics: (i) CDs with hydrophobic cavities can encapsulate hydrophobic drug, while ZIF-8 can serve as reservoirs for loading hydrophilic drug molecules, (ii) strong NIR absorption of PDA chains results in high photothermal conversion capacity from laser energy to heat, (iii) H-ZIF-8/PDA-CD JNPs are featured with pH/NIR dual-responsive drug release behaviors due to the presence of pH-sensitive ZIF-8 nanoparticles, and (iv) the cytotoxicity tests as well as histological and biochemical blood assays all prove the high biocompatibility of the proposed hybrid nanostructure (Fig. 8.5C, c-h). Although this report was the first one to introduce the construction of MOF-polymer nanoparticles for synergetic dual-drug chemo- and photothermal therapy, it promised the potential of MOF-based hybrid materials for further therapeutic-imaging applications.

Recently, Li et al. have designed an endogenous H_2S-activated Cu-MOF (HKUST-1) nanoenzyme for synergic NIR PTT and chemodynamic therapy (CDT) for colon cancer treatment (Li et al., 2020). It has been long found that the dysregulated H_2S production from the catalysis process of overexpressed cystathionine β-synthase (CBS) can be utilized as a specific target for early diagnosis of some certain cancers such as colon and ovarian. Accordingly, the transformation of non-photoactive HKUST-1 nanoenzyme into an NIR-activatable copper sulfide which was triggered by endogenous H_2S species produced from in situ sulfidation reaction was adopted for construction of a smart theranostics nanoplatform for synergic colon cancer treatment.

As schematically illustrated in Fig. 8.5D, for photothermal therapy, an "ON-OFF" strategy was used therein in which the non-photoactive HKUST-1 nanoparticles are in their "OFF" state in normal tissues with no obvious adsorption within the NIR region. This is while near the microenvironment of colon tumor tissues they turned into "ON" state as a consequence of reacting with overexpressed endogenous H_2S and in situ production of photoactive CuS as a photothermal agent with stronger UV-Vis absorption. On the other hand, the prepared HKUST-1 nanoparticles are favorable for CDT due to their horseradish peroxidase (HRP)-mimicking activity which can provoke the effective conversion of overexpressed H_2O_2 within cancer cells into more toxic OH radicals.

Altogether, various strategies and approaches can be applied using MOF-based nanoarchitectures for the design and fabrication of smart therapeutic systems capable of targeting tumor sites and enhance the therapeutic efficacy while reducing the side effects.

8.3.3 Nanoscale MOFs for Cancer Theranostics

As mentioned previously, the design and fabrication of platforms which can potentially integrate therapeutic and diagnostic features in a single platform is of great significance. The versatility of MOFs and their high potential for multifunctionality have turned them swiftly into promising candidates for such theranostics applications. In this regard, theranostic MOFs have developed rapidly, and it is anticipated that these systems play an important role in personalized medicine in the near future. Advantages of nanoscale MOFs for tumor theranostics include desirable biocompatibility, high drug loading capacity, active tumor targeting, and image-guided smart drug delivery. Using these characteristics allows managing the treatment process through monitoring the biodistribution and accumulation of drugs, controlling their release and dose adjustment to patients (Lu et al., 2018; Wu & Yang, 2017).

For any biomedical investigation, in vivo toxicity is a key factor which should be taken into consideration. Accordingly, one of the main goals of developing theranostic nMOFs is to design a low-toxicity nanosystem in the body. To reach this goal, it is important to select appropriate metal centers and organic ligands that both show adequate biocompatibility. In 2015, Maspoch group found out a direct correlation between the in vitro cytotoxicity with that of in vivo toxicity of 16 representative uncoated nMOFs using powder X-ray diffraction and ICP-OES quantification of the corresponding metal ions in the solutions upon incubation at 37 °C (Ruyra et al., 2015). They systematically investigated the stability of nMOFs in the culture medium as well as their in vitro cytotoxicity to HepG2 and MCF7 cells along with their in vivo toxicity in zebrafish (*Danio rerio*) embryos. Their results revealed that certain MOFs including UiO-66 and UiO-67, MIL-100 and MIL-101, and ZIF-7 were mostly stable even after 24 h of incubation, while others such as ZIF-8 and some of MOF-74 nMOFs showed slight degradation; however their respective crystal structures remained unaltered. Some special nMOFs (i.e., MOF-5, HKUST-1, NOTT-100, and most of MOF-74 nMOFs) exhibited great degradation accompanied by a loss of crystallinity. Based on these findings, the authors suggested that the toxicity of nMOFs is strongly related to the toxicity of their metallic nodes and organic ligands which are released into the media upon the degradation of nMOFs. This is while numerous studies have demonstrated that metals such as Ca, Mg, Zn, Fe, Ti, or Zr have safe toxicity as estimated by oral lethal dose 50 (LD50) (Imaz et al., 2010).

Besides, in order to decrease the cytotoxicity and endow the biological compatibility to these porous materials, biological MOFs, also called "BioMOFs," can be utilized. BioMOFs are a class of metal-organic frameworks in which biomolecules such as amino acids, proteins, peptides, nucleobases, carbohydrates, cyclodextrins, and porphyrin (or metalloporphyrin) are used as bio-ligands instead of organic linkers (Imaz et al., 2011; Rojas et al., 2017; Cai et al., 2019).

In the following sections, the various nMOF systems used for theranostic purposes will be discussed in detail. For better understanding, nanoMOF theranostic systems were categorized into iron, zinc, copper, and manganese-based MOFs.

8.3.3.1 Iron-Based MOFs

Nontoxic iron (III) carboxylate metal-organic framework (Fig. 8.6A) is one of the promising subclass of nMOFs which has been widely explored in the theranostic field owing to their biocompatibility and high loading capacities. Moreover, their iron-based core with good relaxivity makes them applicable as a suitable magnetic resonance imaging contrast agent. These properties along with the potential of co-incorporating the therapeutic and diagnostic agents open up new opportunities for smoothing the way for theranostic purposes (Liu et al., 2020).

In 2009, amino-modified iron terephthalate MIL-101 nanoparticles were used to load an anticancer drug (i.e., ethoxysuccinato-cisplatin (ESCP) prodrug) and an organic fluorophore via covalent modifications of the as-prepared nanoparticles, then covered with silica shell to increase the stability as well as enhance the controlled-release property. The adopted post-synthetic modification strategy of highly porous nMOFs provided a platform for optical imaging and anticancer therapy to obtain theranostic purposes (Taylor-Pashow et al., 2009). Horcajada et al. investigated the efficiency of various MIL MOF nanoparticles synthesized through green chemistry (in aqueous or ethanolic solutions) as nontoxic and biocompatible drug nanocarriers (Horcajada et al., 2010). For this purpose, porous MILs with engineered cores and surfaces were loaded with different anticancer or antiviral drugs, namely, busulfan (Bu), azidothymidine triphosphate (AZT-TP), cidofovir (CDV), and doxorubicin (DOX). The results revealed that the prepared nanoMOFs act as remarkable *molecular sponges* capable of encapsulating drugs with different polarities, sizes, and functional groups through simple immersion in the corresponding solutions. Furthermore, they came up with good magnetic resonance imaging properties due to the presence of paramagnetic iron atoms with good relaxivities in their matrix. Another work displayed a functionalized MOF through post-synthetic modification designed for cancer cell imaging and dual chemo-photodynamic therapy (Liu et al., 2017). Camptothecin drug was encapsulated into iron(iii) carboxylate MOFs (NH_2-MIL-101(Fe)) and then integrated with folic acid as targeting moiety as well as chlorine e6-labeled peptide (Ce6-peptide) as a diagnostic agent. The detachment of Ce6-peptide from the MOF surface as a result of its specific cleavage reaction with intracellular cathepsin B (CaB) recovered the fluorescence of Ce6. This CaB-activable fluorescence property was used as a signal switch for imaging applications, while combining Ce6 as the photosensitizer with the camptothecin drug made it operational for chemo-photodynamic dual therapy. Likewise, MIL-88B nanoparticles were loaded with curcumin (Cur) as a hydrophobic anticancer drug followed by coating with folic acid-chitosan conjugate (FC) on the surface of the carrier via electrostatic interactions to attain smart targeted cancer therapy properties (Dehghani et al., 2020). The prepared multifunctional MIL-Cur@FC nanoparticle exhibited simultaneous noninvasive cancer diagnosis with enhanced dual contrast T_1- and T_2-weighted MR imaging features owing to its pH-responsive MRI characteristic due to the degradation of framework in the mild acidic microenvironment of tumor as well as efficient cancer treatment properties through efficient intracellular anticancer drug delivery.

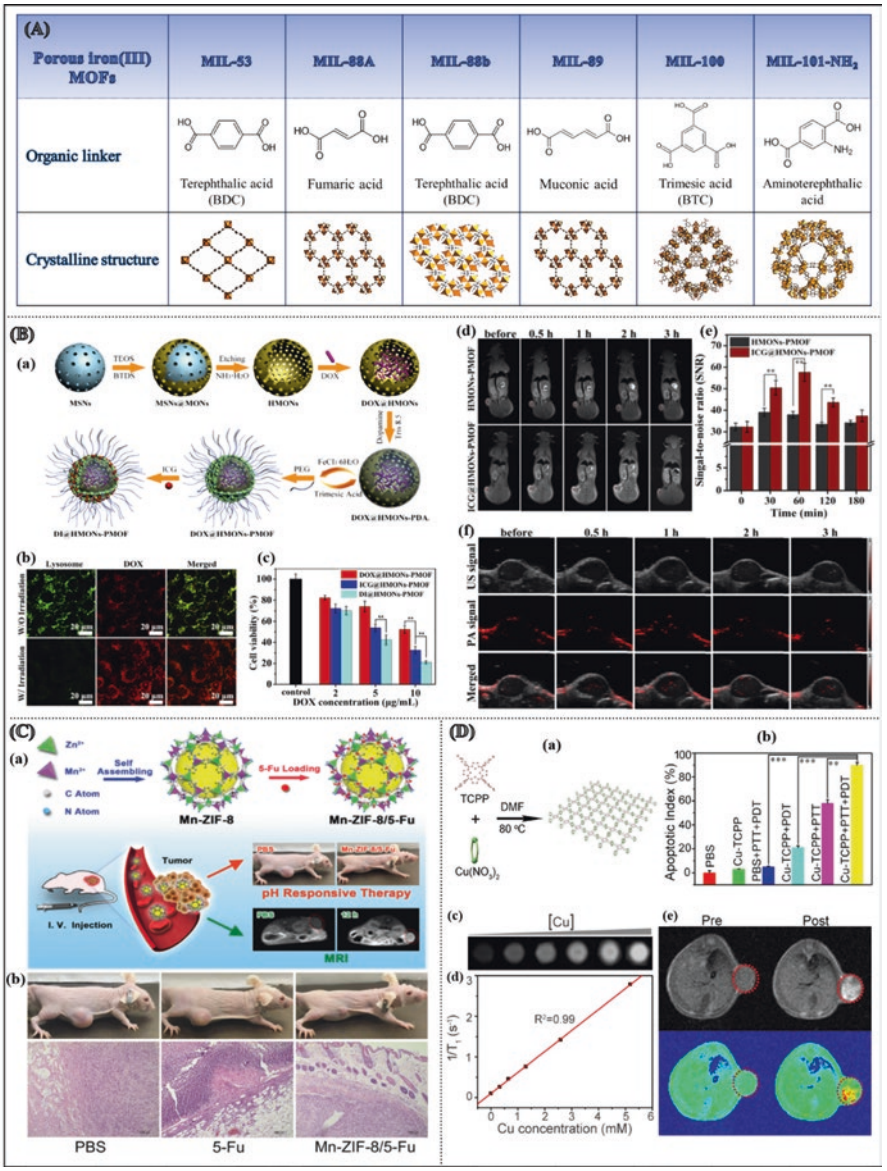

Fig. 8.6 Theranostic MOF nanoplatforms used for imaging-guided cancer therapy; (**A**) Structural description of MIL family composed of iron (III) metal nodes, (**B**) Schematic representation of general procedure of fabricating dual drug-loaded HMONs-PMOF nanoplatform (a), The CLSM images of lysosome-stained 4T1 cells exposed to DI@HMONs-PMOF for 2 h with or without laser irradiation (b), Cell viability of 4T1 cells subjected to chemotherapy and PT therapy alone and the combination therapy (c), MR images (d) and the corresponding signal-to-noise value of tumor-bearing mice at different time intervals of HMONs-PMOF and ICG@HMONs-PMOF post-injection (e), PA images at the tumor site obtained from the tumor-bearing mice in different time intervals of post-injection of ICG@HMONs-PMOF (f) (*Reprinted with permission from* Chen

(continued)

et al. (2019c)), (**C**) Synthetic procedure of Mn-ZIF-8/5-Fu with the application in targeted therapy and MR imaging for glioma (a), H&E staining sections of tumor tissues 14 days after treatment (*Reprinted with permission from* Pan et al. (2019)), (**D**) Schematic illustration of the synthesis process of Cu-TCPP MOF (a), Cancer cell apoptosis after treatment with Cu-TCPP MOF nanosheets (P values: $***p < 0.001$, $**p < 0.01$, or $*p < 0.05$) (b), In vitro T_1-weighted MR images of the Cu-TCPP MOF nanosheets with different concentrations (c) and the corresponding plots of the $1/T_1$ value of the Cu-TCPP MOF nanosheets as a function of concentration (d), *In vivo* T_1-weighted MR views of a mouse before and after intra-tumoral injection of the Cu-TCPP MOF nanosheets solution (e) (*Reprinted with permission from* Li et al. (2018c))

Additionally, the integration of metal-organic frameworks with other functional nanomaterials has resulted in nanoformulations with superior properties and synergistic performance which is not available from any of these nanostructures alone. In this regard, a well-defined hollow structure was formed by successful merging of MOF(Fe) with hollow mesoporous organosilica nanoparticles (HMONs) using a thin layer of polydopamine (PDA) (Chen et al., 2019c). The resulting molecularly organic/inorganic hybridized nanocomposite (HMONs-PMOF) with extraordinary loading capacity (resulted from large cavity of HMONs along with highly porous network of metal-organic framework) was exploited as a nanocontainer inside which the doxorubicin hydrochloride (DOX) drug was loaded. In the meantime, indocyanine green (ICG) with the ability of cooperatively enhancing the MR imaging capability was bound to the outer porous shell of MOF with high loading efficacy. The fabrication process of the dual drug-loaded nanocomposite (DI@HMONs-PMOF) is schematically shown in Fig. 8.6B-a. The killing efficacy of DI@HMONs-PMOF nanocomposite toward cancer cells arose from not only the presence of the chemotherapeutic drug (DOX) that exhibited a pH/NIR laser dual-responsive intracellular release behavior but also the incorporated ICG which provided reasonable photothermal effect and photostability. Moreover, the prepared nanoarchitecture revealed desirable magnetic resonance (MR) and photoacoustic (PA) dual-modality imaging properties benefited from the coordination interaction of iron ions and PDA interlayer as MRI contrast agent as well as the ICG shell with PA imaging capability. Hence, simultaneous chemo-photothermal combination therapy and MR/PA dual-modality imaging were realized with the aid of the prepared nanoplatform with favorable biocompatibility (Fig. 8.6B, b-f).

Conducting polymer-MOF composite/hybrid nanostructures are another intriguing option for nanotheranostic applications. For instance, Zhu and coworkers have proposed a core-shell structure composed of uniform polypyrrole (PPy) nanoparticles with adequate biodegradability as core covered with a mesoporous MIL-100 shell (Zhu et al., 2016). The PPy@MIL-100 composite showed synergistically enhanced therapeutic efficacy by the combination of chemotherapy and PTT. The results were attributed to the high loading capacity of porous MIL shell as DOX drug nanocarrier which exhibited a pH-controlled drug release behavior as well as the role of PPy core as an organic photothermal agent under NIR irradiation.

In another research work, PPy@MIL-53 nanocomposite was prepared through in situ growth of PPy nanoparticles inside MIL-53 MOF as a microreactor in which Fe^{3+} ions played the role of an intrinsic oxidizing agent for polymerizing pyrrole

monomers to PPy nanoparticles (Huang et al., 2018). PPy@MIL-53 nanocomposite integrated the intrinsic photothermal therapy (PTT) of PPy nanoparticles with MR imaging ability of Fe^{3+}. As a consequence, the prepared nanocomposite presented in vitro and in vivo tools for MRI-guided photothermal therapy of cancer. The integration of diagnostic and therapeutic agents was also observed in the core-shell structure of PB@MIL-100(Fe) dual MOFs nanoparticles (dMOFs) (Wang et al., 2016). dMOFs were prepared by layer-by-layer deposition of MIL-100(Fe) MOF shell on the surface of Prussian blue nanocubes and were shown to be useful as a T_1-T_2 dual-modal MRI and fluorescence optical imaging agent. The inner PB core was advantageous for imaging and phototherapy due to strong absorbance in the NIR region, while the porous MOF shell provided great potential for targeted intracellular artemisinin drug delivery as a result of its pH-responsive degradation nature in the acidic pH of lysosomes in the tumor microenvironment.

8.3.3.2 Zinc-Based MOFs

ZIF-8 nanoparticles which are composed of Zn^{2+} ions and 2-methylimidazole (2-MIm) ligands are among the most widely used metal-organic frameworks due to their ease of synthesis via a wide range of methods, excellent in vivo stability and structural robustness, pH responsiveness, as well as high porosity. In this regard, numerous studies have focused on the use of ZIF-8 hybrid nanomaterials for cancer theranostics (He et al., 2014; Li et al., 2018b; Pan et al., 2019; Zhu et al., 2019a; Chowdhuri et al., 2016; Zhu et al., 2019b; Nejadshafiee et al., 2019). He et al. utilized encapsulated fluorescent carbon nanodots (C-dots) in porous ZIF-8 nanoparticles (C-dots@ZIF-8) as a platform for simultaneous pH-responsive anticancer drug delivery and cell fluorescence imaging (He et al., 2014). The encapsulated C-dots, as a new class of nanocarbons which present strong fluorescence intensity, paved the way for fluorescence imaging of cancer cells, while ZIF-8 porous network was exploited as a potential carrier for the loading of 5-fluorouracil (5-Fu) as a representative anticancer drug. In another study, Cy@ZIF-8 nanoparticles were obtained by loading cyanine (Cy) as a NIR-active dye into the zeolitic imidazolate framework-8, and the resulting nanoparticles were used for NIR imaging-guided photothermal therapy (Li et al., 2018b). Cy@ZIF-8 nanoparticles showed notable cytotoxicity toward cancer cells under a specific wavelength of laser with an increase of Cy concentration. Moreover, in order to assess the antitumor efficacy of the system, NIR fluorescence imaging was performed using calcein AM and propidium iodide. The results demonstrated that Cy@ZIF-8 nanoparticles were mostly located in the tumor and liver. Altogether, the prepared Cy@ZIF-8 composite demonstrated NIR absorbance, photothermal transformation, and NIR imaging capability which made it suitable for theranostic applications.

Determination of tumor uptake and diagnosis of glioma rely on the MRI results as a recognition method for detecting tumor anatomical details with high quality. In a research conducted by Pan and coworkers, the bimetallic zeolitic imidazolate framework (Mn-ZIF-8) was used as a drug delivery system of 5-Fu and applied for

the first time for in vivo magnetic resonance imaging (Pan et al., 2019). As schematically illustrated in Fig. 8.6C-a, the synthesized Mn-ZIF-8/5-Fu nanoparticles were served as a multifunctional theranostic nanomedical platform which combined the MR imaging capability of accumulated Mn^{2+} in the tumor sites, ultrahigh antiglioma drug loading into ZIF-8 nanoparticles with high specific surface area, and pH-responsive drug release in a single system. The hematoxylin and eosin (H&E) staining sections of tumor tissues obtaining 14 days after treatment are shown in Fig. 8.6C-b. As can be seen, excellent therapeutic effects and prolonged survival time was obtained for the Mn-ZIF-8/5-Fu group. These observations were attributed to the augmented drug concentrations in the tumors as a result of longer circulation time of blood with higher concentration of drug. Another ZIF-8 multifunctional MOF with the composition of DOX/Pd@ZIF-8 was also constructed as a theranostic nanoplatform (Zhu et al., 2019a). The fabricated nanosystem indicated photothermal and optoacoustic effects due to the high NIR absorption of Pd nanoparticles loaded into MOFs. Also, DOX showed a pH-dependent release that enabled successful chemotherapy.

Zn-based nMOFs other than ZIF-8 were also investigated for theranostic applications. As an example, magnetic Fe_3O_4@IRMOF-3 nanostructures were fabricated by the incorporation of Fe_3O_4 nanoparticles into isoreticular metal organic frameworks (IRMOF-3) and used as the first targeted magnetic nMOFs for the delivery of hydrophobic drugs and MR imaging (Chowdhuri et al., 2016). Fe_3O_4 is a T_2 contrast agent for magnetic resonance imaging. Furthermore, rhodamine B isothiocyanate (RITC) was conjugated to the nMOFs as the fluorescent agent for biomedical imaging. As an anticancer drug, paclitaxel was incorporated into the prepared nanocarriers with high loading capacity. Finally, folic acid was conjugated to the surface of nMOFs to obtain a targeted drug delivery system. Two-dimensional nMOFs with much larger surface area compared to their particulate counterparts are another emerging class of MOFs with attractive features for theranostic purposes. For instance, 2D nanosheets based on Zn^{2+} metal centers and tetrakis (4-carboxyphenyl) porphyrin (TCPP) organic linkers were synthesized and further functionalized with polyethylene glycol (PEG) (Zhu et al., 2019b). The Zn-TCPP@PEG nanoparticles not only exhibited enhanced photodynamic therapeutic effect due to the more efficient light-triggered singlet oxygen production but also showed higher drug loading capacity for DOX chemotherapy drugs as a result of their sheet structure. The porphyrin structure of TCPP made it possible for the 2D nMOFs to be labeled with ^{99m}Tc as a diagnostic radioisotope and consequently used for single photon emission computed tomography (SPECT) imaging. It is noteworthy to mention that the prepared nanosheets showed efficient antitumor chemo-PDT effect with low biotoxicity which results from their rapid renal clearance. Similarly, another magnetic metal-organic framework, namely, Fe_3O_4@Bio-MOF, which was coated with folic acid and conjugated with chitosan (FC) was also reported for delivery of curcumin (Cur) and 5-fluorouracil (5-FU) in cancer targeted therapy (Nejadshafiee et al., 2019). In this study, MOF nanocarriers loaded by anticancer drugs demonstrated high toxicity against the cancer cells. MRI investigations indicated negative signal improvement in the in vitro and in vivo tumor studies, which revealed the capability

of using the nanoparticles as a diagnostic agent. Accordingly, the performance of these nanocarriers in T_2 MRI and their cytotoxicity effect on cancer cells proved the potential of these nMOFs as promising agents in cancer theranostics.

8.3.3.3 Cu- and Mn-Based MOFs

Cu-containing MOFs have attracted a great deal of attention during the past few years due to their inherent properties: (i) Cu^{2+} sites show strong binding attraction to some anions such as S^{2-} which present in high concentration in some certain cancer as a result of high overexpression of H_2S in the tumor microenvironment, (ii) Cu-MOFs are convenient for chemodynamic therapy (CDT) since they exhibit peroxidase-mimicking activity which can catalyze the formation of toxic hydroxyl radicals (•OH) from H_2O_2 secreted by cancer cells, and (iii) compared to Fe^{2+}, the Cu^{2+}/Cu^{+} pair has lower redox potential (~0.16 eV) and, as a result, offers higher catalytic activity as Fenton agents (Li et al., 2020; Ma et al., 2018; Zhang et al., 2018b; Ke et al., 2011; Li et al., 2018c). HKUST-1 MOF, which is composed of dimeric copper metal units connected by benzene-1,3,5-tricarboxylate (BTC) linker molecules, is an example of appropriate nMOFs for theranostics purposes (Li et al., 2020; Ke et al., 2011). In 2011, a magnetic Cu-based MOF composite was prepared via incorporation of Fe_3O_4 nanorods with nanocrystals of HKUST-1 (Fe_3O_4/$Cu_3(BTC)_2$) and was further investigated for targeted delivery of nimesulide (NIM) as an anticancer drug for pancreatic cancer treatment along with MR imaging (Ke et al., 2011). The prepared three-dimensional MOF with a 3D channel system showed high loading capacity (up to 0.2 g of NIM) due to its extraordinary porosity as well as prolonged release duration of as long as 11 days in physiological saline at 37 °C. This theranostic nanoplatform was one of the very first examples of MOF materials for targeted drug delivery goals.

Copper-tetrakis (4-carboxyphenyl) porphyrin (Cu-TCPP) nanosheet (Fig. 8.6D-a) is another example which not only exhibited strong NIR absorption and capability for magnetic resonance imaging as a result of copper centers but also showed synergistic effect of photothermal and photodynamic therapy due to the presence of TCCP with the ability of producing singlet oxygen (SO) as a characteristic photosensitizer (Li et al., 2018c). Two-dimensional (2D) nanosheets demonstrated better photothermal effect than bulk materials because of more rapid response to light. As can be seen in Fig. 8.6D-b which shows the cancer cell apoptosis, the cell mortality rates for the Cu-TCPP under PDT and the Cu-TCPP group under PTT were ~21% and ~58%, respectively. This is while for the cells treated with Cu-TCPP MOF under PD/PTT condition, the cell mortality demonstrated a remarkable increase up to ~90%. The obtained combination index (CI) of 0.778 revealed the synergetic PDT/PTT effect which is originated from the photosensitizing effect of TCPP capable of generating toxic singlet oxygen for PDT plus the ability of converting light energy into heat under NIR irradiation for PTT that cause hyperthermia in the tumor environment. In addition, these nanosheets showed T_1-weighted MR imaging ability due to the unpaired 3D electrons in copper. The in vitro and in vivo MR images are

shown in Fig. 8.6D, c-e which illustrate a sharp color contrast after injection of MOF nanosheets compared with that of before injection. The obtained results confirmed that ultrathin Cu-TCPP MOF nanosheets could be utilized as a theranostic agent for imaging and phototherapy of cancer.

Mn-based nMOFs present another interesting nanoplatforms for bioimaging implementations due to the ability of Mn^{2+} ions as an efficient T_1-weighted contrast agent when binding to intracellular proteins (Wang et al., 2018b; Liu et al., 2014b; Zhao et al., 2017). Theranostic features were observed in a multifunctional Mn-containing nanoscale coordination polymer as a result of high capacity for loading an anticancer agent (zoledronate) along with the presence of Mn^{2+} centers as MRI contrast agent (Liu et al., 2014b). Surface pegylation followed by functionalization with anisamide as a targeting group was adopted to control the kinetics of the drug release and to endow the specificity to cancer cells, respectively. The results demonstrated the ability of the as-prepared Mn-bisphosphonate particles with physiological stability and biocompatibility for imaging-guided targeted cancer therapy. Intelligent and logical design of nMOF structures is a key parameter in obtaining the desired results. As an example, a redox-sensitive MOF was synthesized from Mn^{2+} nodes and dithiodiglycolic acid as the disulfide (SS)-containing organic ligand (Zhao et al., 2017). The yielded nanoparticles were loaded with DOX and then coated with a PDA layer. In such a redox-active structure, the release of drug can be triggered by the cleavage of disulfide bonds (S-S) within dithiodiglycolic acid in the presence of excessive glutathione (GSH) and the subsequent decomposition of MOF. This is while the manganese centers offer a strong T_1 contrast in MRI. Similar strategies can be adopted for constructing various stimuli-responsive theranostic nanoplatforms susceptible to different exogenous and/or endogenous environmental stimuli such as pH, reactive oxygen species, and even light and temperature.

8.3.3.4 Other MOFs

Apart from the aforementioned transition metals which were widely used in the construction of theranostic nMOFs, certain frameworks with unusual metallic centers were also reported (Zhang et al., 2018a; Meng et al., 2020; Rowe et al., 2009).

A novel biocompatible MOF composed of UiO-66 (Zr) with carboxylic acid (COOH) groups was incorporated with Mn^{2+} and doxorubicin as diagnostic and therapeutic compounds, respectively (Meng et al., 2020). The prepared multifunctional MOF-based nanosystem showed promoted T_1-weighted relaxivity and pH-responsive drug release. The simultaneous incorporation of diagnosis and therapeutic agents led into a platform with the ability of tracing the accumulation of nanoparticles, assisted in diagnosis, allowing evaluation of therapy through magnetic resonance imaging along with eradicating tumor cells by the aid of doxorubicin. Mn^{2+}-DOX@MOF showed significant dose-dependent cytotoxicity for breast cancer and demonstrated high survival rate for lung metastasis as well. The MR images exhibited high sensitivity of Mn^{2+}-DOX@MOF in probing tumors and the potential for tumor detection of the fabricated nanocarrier.

As another MOFs for theranostic applications, polymer-modified Gd(III) nMOFs were introduced as a multifunctional device (Rowe et al., 2009). In this research, the surface of Gd MOF nanoparticles was modified for the first time with biocompatible polymers. These nMOFs were loaded with anticancer drug methotrexate (MTX) and then functionalized with a fluorescent dye and targeting peptide. The modified nMOFs exhibited bimodal imaging ability (fluorescence and MRI). The incorporation of FMA (fluorescein-O-methacrylate) into the backbone of the copolymer allowed the cellular level imaging via fluorescence microscopy. On the other hand, the Gd centers acted as a contrast agent for MRI. These two features could provide diagnostic imaging at the clinical level accompanied by treatment through MTX.

Furthermore, MOFs could be also used in X-ray computed tomography imaging as mentioned previously. For example, Yb-MOFs-Glu with 3-dicarboxylic acid (BBDC) as ligand and glucose as a biocompatibility enhancer provided a platform for CT imaging. Yb is an element with a high molecular weight that exhibited X-ray attenuation. Thus, DOX@Yb-MOFs-Glu indicated great potential for chemotherapy and CT imaging and represented theranostic capability (Zhang et al., 2018a).

8.4 Future Perspectives and Conclusion

Since their discovery in 1989, MOFs have attracted a great deal of attention not only as a result of their versatile molecular architectures and topologies but also due to their wide range of applications. Compared to advanced composites and hybrid materials, MOFs present both properties of being prepared in a single step via various strategies and by simply mixing the components as well as the ability of tuning the structural features through controlling the reaction conditions (i.e., temperature, solvent polarity, pressure, the presence of additives, the concentration of metal salts/organic linkers, and their ratio). Furthermore, a wide variety of secondary building units (SBUs) and on-demand synthesized organic linkers can be introduced to provide the scientific community with infinite properties. Therefore, the past few years have witnessed an increasing development in the exploitation of MOFs for diverse applications including bioimaging, drug delivery, and diagnosis purposes. Their beneficial characteristics such as tunable porosity, ease of surface modification, biocompatibility, biodegradability, bioavailability, high drug loading capacity, and controlled release manner have paved the way for their utilization in cancer theranostics which potentially integrate therapeutic and diagnostic features in a single platform. In this regard, MOFs are considered as promising nanomedical systems for cancer theranostic applications in order to achieve a faster diagnosis and more efficient treatment of cancer. As a result, theranostic nanoMOFs have developed rapidly, and it is expected that these systems play a vital role in personalized medicine in the near future. However, there are limitations such as low selectivity and high cost of certain organic ligands that should be considered to improve the efficacy of MOFs as theranostic platforms. The in vitro and in vivo stability of nanoMOFs against degradation and aggregation stay still challenging and need to be investigated. Their

degradation behavior, the toxicity of the components, as well as the possible elimination roots from the body should be well identified for their further development as theranostic systems. New MOFs can be engineered for biomedical applications by gaining in-depth knowledge on their degradation behavior in biological fluids. For MOFs to be applied in real biomedicine and clinical use, their biodistribution, efficacy, health risks, in vitro/in vivo biosafety, and environmental issues have to be investigated in more detail. More emphasis should be paid on the optimization and design of safe and stable multifunctional stimuli-responsive nanoMOFs based on green, environmentally friendly, and energy-efficient approaches with demonstration of sufficient biodegradability and biocompatibility of the as-prepared nanoparticles. Although there exists many challenges and further progress is still needed for practical applications, MOFs are still attractive candidates with a bright future and promising capabilities in various fields owing to their outstanding properties. Hence, it is anticipated that an increasing number of researches will appear in the near future exploiting the full potential of nanoMOFs in various biomedical fields.

References

Abdollahi, N., Masoomi, M. Y., Morsali, A., Junk, P. C., & Wang, J. (2018). Sonochemical synthesis and structural characterization of a new Zn (II) nanoplate metal-organic framework with removal efficiency of Sudan red and Congo red. *Ultrasonics Sonochemistry, 45*, 50–56.

Al Amery, N., Abid, H. R., Al-Saadi, S., Wang, S., & Liu, S. (2020). Facile directions for synthesis, modification and activation of MOFs. *Materials Today Chemistry, 17*, 100343.

Alexis, F., Pridgen, E., Molnar, L. K., & Farokhzad, O. C. (2008). Factors affecting the clearance and biodistribution of polymeric nanoparticles. *Molecular Pharmaceutics, 5*(4), 505–515.

Al-Kutubi, H., Gascon, J., Sudhölter, E. J., & Rassaei, L. (2015). Electrosynthesis of metal-organic frameworks: Challenges and opportunities. *ChemElectroChem, 2*(4), 462–474.

Amini, A., Kazemi, S., & Safarifard, V. (2020). Metal-organic framework-based nanocomposites for sensing applications – A review. *Polyhedron, 177*, 114260.

Armstrong, M. R., Senthilnathan, S., Balzer, C. J., Shan, B., Chen, L., & Mu, B. (2017). Particle size studies to reveal crystallization mechanisms of the metal organic framework HKUST-1 during sonochemical synthesis. *Ultrasonics Sonochemistry, 34*, 365–370.

Asadian, E., Shahrokhian, S., & Zad, A. I. (2020). ZIF-8/PEDOT@flexible carbon cloth electrode as highly efficient electrocatalyst for oxygen reduction reaction. *International Journal of Hydrogen Energy, 45*(3), 1890–1900.

Babu, R., Roshan, R., Kathalikkattil, A. C., Kim, D. W., & Park, D. W. (2016). Rapid, microwave-assisted synthesis of cubic, three-dimensional, highly porous MOF-205 for room temperature CO_2 fixation via cyclic carbonate synthesis. *ACS Applied Materials & Interfaces, 8*(49), 33723–33731.

Biswal, B. P., Chandra, S., Kandambeth, S., Lukose, B., Heine, T., & Banerjee, R. (2013). Mechanochemical synthesis of chemically stable isoreticular covalent organic frameworks. *Journal of the American Chemical Society, 135*(14), 5328–5331.

Boddula, R., Ahamed, M. I., & Asiri, A. M. (Eds.). (2020). *Applications of metal-organic frameworks and their derived materials*. John Wiley & Sons.

Cai, W., Chu, C. C., Liu, G., & Wáng, Y. X. J. (2015). Metal-organic framework-based nanomedicine platforms for drug delivery and molecular imaging. *Small, 11*(37), 4806–4822.

Cai, W., Gao, H., Chu, C., Wang, X., Wang, J., Zhang, P., Lin, G., Li, W., Liu, G., & Chen, X. (2017). Engineering photo-theranostic nanoscale metal-organic frameworks for multimodal imaging-guided cancer therapy. *ACS Applied Materials & Interfaces, 9*(3), 2040–2051.

Cai, H., Huang, Y. L., & Li, D. (2019). Biological metal-organic frameworks: Structures, host–guest chemistry and bio-applications. *Coordination Chemistry Reviews, 378*, 207–221.

Campagnol, N., Van Assche, T. R., Li, M., Stappers, L., Dincă, M., Denayer, J. F., Binnemans, K., De Vos, D. E., & Fransaer, J. (2016). On the electrochemical deposition of metal-organic frameworks. *Journal of Materials Chemistry A, 4*(10), 3914–3925.

Cao, X., Zheng, B., Rui, X., Shi, W., Yan, Q., & Zhang, H. (2014). Metal oxide-coated three-dimensional graphene prepared by the use of metal–organic frameworks as precursors. *Angewandte Chemie International Edition, 53*(5), 1404–1409.

Cao, J., Li, X., & Tian, H. (2020). Metal-organic framework (MOF)-based drug delivery. *Current Medicinal Chemistry, 27*(35), 5949–5969.

Chalati, T., Horcajada, P., Gref, R., Couvreur, P., & Serre, C. (2011). Optimization of the synthesis of MOF nanoparticles made of flexible porous iron fumarate MIL-88A. *Journal of Materials Chemistry, 21*(7), 2220–2227.

Chen, D., Yang, D., Dougherty, C. A., Lu, W., Wu, H., He, X., Cai, T., Van Dort, M. E., Ross, B. D., & Hong, H. (2017). In vivo targeting and positron emission tomography imaging of tumor with intrinsically radioactive metal-organic frameworks nanomaterials. *ACS Nano, 11*(4), 4315–4327.

Chen, C., Feng, X., Zhu, Q., Dong, R., Yang, R., Cheng, Y., & He, C. (2019a). Microwave-assisted rapid synthesis of well-shaped MOF-74 (Ni) for CO_2 efficient capture. *Inorganic Chemistry, 58*(4), 2717–2728.

Chen, D., Zhao, J., Zhang, P., & Dai, S. (2019b). Mechanochemical synthesis of metal-organic frameworks. *Polyhedron, 162*, 59–64.

Chen, L., Zhang, J., Zhou, X., Yang, S., Zhang, Q., Wang, W., You, Z., Peng, C., & He, C. (2019c). Merging metal organic framework with hollow organosilica nanoparticles as a versatile nano-platform for cancer theranostics. *Acta Biomaterialia, 86*, 406–415.

Chen, L., Zhang, X., Cheng, X., Xie, Z., Kuang, Q., & Zheng, L. (2020). The function of metal-organic frameworks in the application of MOF-based composites. *Nanoscale Advances, 2*, 2628–2647.

Cheng, X., Zhang, A., Hou, K., Liu, M., Wang, Y., Song, C., Zhang, G., & Guo, X. (2013). Size- and morphology-controlled NH_2-MIL-53 (Al) prepared in DMF-water mixed solvents. *Dalton Transactions, 42*(37), 13698–13705.

Cheng, G., Li, W., Ha, L., Han, X., Hao, S., Wan, Y., Wang, Z., Dong, F., Zou, X., Mao, Y., & Zheng, S. Y. (2018). Self-assembly of extracellular vesicle-like metal-organic framework nanoparticles for protection and intracellular delivery of biofunctional proteins. *Journal of the American Chemical Society, 140*(23), 7282–7291.

Cho, K., Wang, X. U., Nie, S., & Shin, D. M. (2008). Therapeutic nanoparticles for drug delivery in cancer. *Clinical Cancer Research, 14*(5), 1310–1316.

Cho, H. Y., Yang, D. A., Kim, J., Jeong, S. Y., & Ahn, W. S. (2012). CO_2 adsorption and catalytic application of Co-MOF-74 synthesized by microwave heating. *Catalysis Today, 185*(1), 35–40.

Cho, H. Y., Kim, J., Kim, S. N., & Ahn, W. S. (2013). High yield 1-L scale synthesis of ZIF-8 via a sonochemical route. *Microporous and Mesoporous Materials, 169*, 180–184.

Choi, H. S., & Frangioni, J. V. (2010). Nanoparticles for biomedical imaging: Fundamentals of clinical translation. *Molecular Imaging, 9*(6), 7290–2010.

Choi, J. S., Son, W. J., Kim, J., & Ahn, W. S. (2008). Metal-organic framework MOF-5 prepared by microwave heating: Factors to be considered. *Microporous and Mesoporous Materials, 116*(1–3), 727–731.

Chowdhuri, A. R., Bhattacharya, D., & Sahu, S. K. (2016). Magnetic nanoscale metal organic frameworks for potential targeted anticancer drug delivery, imaging and as an MRI contrast agent. *Dalton Transactions, 45*(7), 2963–2973.

Dadfar, S. M., Roemhild, K., Drude, N. I., von Stillfried, S., Knüchel, R., Kiessling, F., & Lammers, T. (2019). Iron oxide nanoparticles: Diagnostic, therapeutic and theranostic applications. *Advanced Drug Delivery Reviews, 138*, 302–325.

Dastbaz, A., Karimi-Sabet, J., & Moosavian, M. A. (2019). Sonochemical synthesis of novel decorated graphene nanosheets with amine functional Cu-terephthalate MOF for hydrogen adsorption: Effect of ultrasound and graphene content. *International Journal of Hydrogen Energy, 44*(48), 26444–26458.

Dehghani, S., Hosseini, M., Haghgoo, S., Changizi, V., Akbari Javar, H., Khoobi, M., & Riahi Alam, N. (2020). Multifunctional MIL-Cur@FC as a theranostic agent for magnetic resonance imaging and targeting drug delivery: In vitro and in vivo study. *Journal of Drug Targeting, 28*(6), 668–680.

Della Rocca, J., Liu, D., & Lin, W. (2011). Nanoscale metal-organic frameworks for biomedical imaging and drug delivery. *Accounts of Chemical Research, 44*(10), 957–968.

Deng, J., Wang, K., Wang, M., Yu, P., & Mao, L. (2017). Mitochondria targeted nanoscale zeolitic imidazole framework-90 for ATP imaging in live cells. *Journal of the American Chemical Society, 139*(16), 5877–5882.

Dey, C., Kundu, T., Biswal, B. P., Mallick, A., & Banerjee, R. (2014). Crystalline metal-organic frameworks (MOFs): Synthesis, structure and function. *Acta Crystallographica Section B: Structural Science, Crystal Engineering and Materials, 70*(1), 3–10.

Dhainaut, J., Bonneau, M., Ueoka, R., Kanamori, K., & Furukawa, S. (2020). Formulation of metal-organic framework inks for the 3D printing of robust microporous solids toward high-pressure gas storage and separation. *ACS Applied Materials & Interfaces, 12*(9), 10983–10992.

Dolgopolova, E. A., Rice, A. M., Martin, C. R., & Shustova, N. B. (2018). Photochemistry and photophysics of MOFs: Steps towards MOF-based sensing enhancements. *Chemical Society Reviews, 47*(13), 4710–4728.

Dolmans, D. E., Fukumura, D., & Jain, R. K. (2003). Photodynamic therapy for cancer. *Nature Reviews Cancer, 3*(5), 380–387.

Doughty, A. C., Hoover, A. R., Layton, E., Murray, C. K., Howard, E. W., & Chen, W. R. (2019). Nanomaterial applications in photothermal therapy for cancer. *Materials, 12*(5), 779.

Esrafili, L., Tehrani, A. A., Morsali, A., Carlucci, L., & Proserpio, D. M. (2019). Ultrasound and solvothermal synthesis of a new urea-based metal-organic framework as a precursor for fabrication of cadmium (II) oxide nanostructures. *Inorganica Chimica Acta, 484*, 386–393.

Flügel, E. A., Ranft, A., Haase, F., & Lotsch, B. V. (2012). Synthetic routes toward MOF nanomorphologies. *Journal of Materials Chemistry, 22*(20), 10119–10133.

Gharatape, A., & Salehi, R. (2017). Recent progress in theranostic applications of hybrid gold nanoparticles. *European Journal of Medicinal Chemistry, 138*, 221–233.

Guan, Q., Li, Y. A., Li, W. Y., & Dong, Y. B. (2018). Photodynamic therapy based on nanoscale metal-organic frameworks: From material design to cancer nanotherapeutics. *Chemistry–An Asian Journal, 13*(21), 3122–3149.

Gul, S., Khan, S. B., Rehman, I. U., Khan, M. A., & Khan, M. I. (2019). A comprehensive review of magnetic nanomaterials modern day theranostics. *Frontiers in Materials, 6*, 179.

Guo, J., Rahme, K., He, Y., Li, L. L., Holmes, J. D., & O'Driscoll, C. M. (2017). Gold nanoparticles enlighten the future of cancer theranostics. *International Journal of Nanomedicine, 12*, 6131.

Gupta, N., Rai, D. B., Jangid, A. K., & Kulhari, H. (2019). A review of theranostics applications and toxicities of carbon nanomaterials. *Current Drug Metabolism, 20*(6), 506–532.

Han, X., Xu, K., Taratula, O., & Farsad, K. (2019). Applications of nanoparticles in biomedical imaging. *Nanoscale, 11*(3), 799–819.

Haque, E., Khan, N. A., Park, J. H., & Jhung, S. H. (2010). Synthesis of a metal-organic framework material, iron terephthalate, by ultrasound, microwave, and conventional electric heating: A kinetic study. *Chemistry–A European Journal, 16*(3), 1046–1052.

Hauser, J. L., Tso, M., Fitchmun, K., & Oliver, S. R. (2019). Anodic electrodeposition of several metal organic framework thin films on indium tin oxide glass. *Crystal Growth & Design, 19*(4), 2358–2365.

He, L., Wang, T., An, J., Li, X., Zhang, L., Li, L., Li, G., Wu, X., Su, Z., & Wang, C. (2014). Carbon nanodots@ zeolitic imidazolate framework-8 nanoparticles for simultaneous pH-responsive drug delivery and fluorescence imaging. *CrystEngComm, 16*(16), 3259–3263.

Horcajada, P., Chalati, T., Serre, C., Gillet, B., Sebrie, C., Baati, T., Eubank, J. F., Heurtaux, D., Clayette, P., Kreuz, C., & Chang, J. S. (2010). Porous metal-organic-framework nanoscale carriers as a potential platform for drug delivery and imaging. *Nature Materials, 9*(2), 172–178.

Hoskins, B. F., & Robson, R. (1990). Design and construction of a new class of scaffolding-like materials comprising infinite polymeric frameworks of 3D-linked molecular rods. A reappraisal of the zinc cyanide and cadmium cyanide structures and the synthesis and structure of the diamond-related frameworks $[N(CH_3)_4][CuIZnII(CN)_4]$ and CuI [4, 4′, 4″, 4‴-tetracyanotetraphenylmethane]$BF_4.xC_6H_5NO_2$. *Journal of the American Chemical Society, 112*(4), 1546–1554.

Hossen, S., Hossain, M. K., Basher, M. K., Mia, M. N. H., Rahman, M. T., & Uddin, M. J. (2019). Smart nanocarrier-based drug delivery systems for cancer therapy and toxicity studies: A review. *Journal of Advanced Research, 15*, 1–18.

Hu, S., Liu, M., Li, K., Zuo, Y., Zhang, A., Song, C., Zhang, G., & Guo, X. (2014). Solvothermal synthesis of NH_2-MIL-125 (Ti) from circular plate to octahedron. *CrystEngComm, 16*(41), 9645–9650.

Hu, F., Mao, D., Wang, Y., Wu, W., Zhao, D., Kong, D., & Liu, B. (2018). Metal-organic framework as a simple and general inert nanocarrier for photosensitizers to implement activatable photodynamic therapy. *Advanced Functional Materials, 28*(19), 1707519.

Huang, H., & Lovell, J. F. (2017). Advanced functional nanomaterials for theranostics. *Advanced Functional Materials, 27*(2), 1603524.

Huang, J., Li, N., Zhang, C., & Meng, Z. (2018). Metal-organic framework as a microreactor for in situ fabrication of multifunctional nanocomposites for photothermal-chemotherapy of tumors in vivo. *ACS Applied Materials & Interfaces, 10*(45), 38729–38738.

Huxford, R. C., deKrafft, K. E., Boyle, W. S., Liu, D., & Lin, W. (2012). Lipid-coated nanoscale coordination polymers for targeted delivery of antifolates to cancer cells. *Chemical Science, 3*(1), 198–204.

Imaz, I., Rubio-Martínez, M., García-Fernández, L., García, F., Ruiz-Molina, D., Hernando, J., Puntes, V., & Maspoch, D. (2010). Coordination polymer particles as potential drug delivery systems. *Chemical Communications, 46*(26), 4737–4739.

Imaz, I., Rubio-Martínez, M., An, J., Sole-Font, I., Rosi, N. L., & Maspoch, D. (2011). Metal-biomolecule frameworks (MBioFs). *Chemical Communications, 47*(26), 7287–7302.

Indoria, S., Singh, V., & Hsieh, M. F. (2020). Recent advances in theranostic polymeric nanoparticles for cancer treatment: A review. *International Journal of Pharmaceutics, 582*, 119314.

Jhung, S. H., Lee, J. H., & Chang, J. S. (2005). Microwave synthesis of a nanoporous hybrid material, chromium trimesate. *Bulletin of the Korean Chemical Society, 26*(6), 880–881.

Jung, D. W., Yang, D. A., Kim, J., Kim, J., & Ahn, W. S. (2010). Facile synthesis of MOF-177 by a sonochemical method using 1-methyl-2-pyrrolidinone as a solvent. *Dalton Transactions, 39*(11), 2883–2887.

Kalmutzki, M. J., Hanikel, N., & Yaghi, O. M. (2018). Secondary building units as the turning point in the development of the reticular chemistry of MOFs. *Science Advances, 4*(10), eaat9180.

Ke, F., Yuan, Y. P., Qiu, L. G., Shen, Y. H., Xie, A. J., Zhu, J. F., Tian, X. Y., & Zhang, L. D. (2011). Facile fabrication of magnetic metal-organic framework nanocomposites for potential targeted drug delivery. *Journal of Materials Chemistry, 21*(11), 3843–3848.

Kepert, C. J., & Rosseinsky, M. J. (1999). Zeolite-like crystal structure of an empty microporous molecular framework. *Chemical Communications, 4*, 375–376.

Khan, N. A., Haque, E., & Jhung, S. H. (2010). Rapid syntheses of a metal-organic framework material $Cu_3(BTC)_2(H_2O)_3$ under microwave: A quantitative analysis of accelerated syntheses. *Physical Chemistry Chemical Physics, 12*(11), 2625–2631.

Kim, J., Yang, S. T., Choi, S. B., Sim, J., Kim, J., & Ahn, W. S. (2011). Control of catenation in CuTATB-n metal–organic frameworks by sonochemical synthesis and its effect on CO_2 adsorption. *Journal of Materials Chemistry, 21*(9), 3070–3076.

Klimakow, M., Klobes, P., Thunemann, A. F., Rademann, K., & Emmerling, F. (2010). Mechanochemical synthesis of metal-organic frameworks: A fast and facile approach toward quantitative yields and high specific surface areas. *Chemistry of Materials, 22*(18), 5216–5221.

Kumar, P., Deep, A., & Kim, K. H. (2015). Metal organic frameworks for sensing applications. *TrAC Trends in Analytical Chemistry, 73*, 39–53.

Lan, G., Ni, K., & Lin, W. (2019). Nanoscale metal-organic frameworks for phototherapy of cancer. *Coordination Chemistry Reviews, 379*, 65–81.

Lee, Y. R., Kim, J., & Ahn, W. S. (2013). Synthesis of metal-organic frameworks: A mini review. *Korean Journal of Chemical Engineering, 30*(9), 1667–1680.

Li, M., & Dincă, M. (2014). Selective formation of biphasic thin films of metal-organic frameworks by potential-controlled cathodic electrodeposition. *Chemical Science, 5*(1), 107–111.

Li, H., Eddaoudi, M., O'Keeffe, M., & Yaghi, O. M. (1999). Design and synthesis of an exceptionally stable and highly porous metal-organic framework. *Nature, 402*(6759), 276–279.

Li, L., Sun, K. K., Fan, L., Hong, W., Xu, Z. S., & Liu, L. (2014). Layer by layer assembly synthesis of Fe_3O_4@ MOFs/GO core–shell nanoparticles. *Materials Letters, 126*, 197–201.

Li, W. J., Tu, M., Cao, R., & Fischer, R. A. (2016a). Metal-organic framework thin films: Electrochemical fabrication techniques and corresponding applications & perspectives. *Journal of Materials Chemistry A, 4*(32), 12356–12369.

Li, Y., Miao, J., Sun, X., Xiao, J., Li, Y., Wang, H., Xia, Q., & Li, Z. (2016b). Mechanochemical synthesis of Cu-BTC@GO with enhanced water stability and toluene adsorption capacity. *Chemical Engineering Journal, 298*, 191–197.

Li, H., Wang, K., Sun, Y., Lollar, C. T., Li, J., & Zhou, H. C. (2018a). Recent advances in gas storage and separation using metal-organic frameworks. *Materials Today, 21*(2), 108–121.

Li, Y., Xu, N., Zhou, J., Zhu, W., Li, L., Dong, M., Yu, H., Wang, L., Liu, W., & Xie, Z. (2018b). Facile synthesis of a metal–organic framework nanocarrier for NIR imaging-guided photothermal therapy. *Biomaterials Science, 6*(11), 2918–2924.

Li, B., Wang, X., Chen, L., Zhou, Y., Dang, W., Chang, J., & Wu, C. (2018c). Ultrathin Cu-TCPP MOF nanosheets: A new theragnostic nanoplatform with magnetic resonance/near-infrared thermal imaging for synergistic phototherapy of cancers. *Theranostics, 8*(15), 4086.

Li, X., Cai, Z., Jiang, L. P., He, Z., & Zhu, J. J. (2019a). Metal-ligand coordination nanomaterials for biomedical imaging. *Bioconjugate Chemistry, 31*(2), 332–339.

Li, S., Zhang, L., Liang, X., Wang, T., Chen, X., Liu, C., Li, L., & Wang, C. (2019b). Tailored synthesis of hollow MOF/polydopamine Janus nanoparticles for synergistic multi-drug chemo-photothermal therapy. *Chemical Engineering Journal, 378*, 122175.

Li, Y., Zhou, J., Wang, L., & Xie, Z. (2020). Endogenous hydrogen sulfide-triggered MOF-based nanoenzyme for synergic cancer therapy. *ACS Applied Materials & Interfaces, 12*(27), 30213–30220.

Liu, D., Kramer, S. A., Huxford-Phillips, R. C., Wang, S., Della Rocca, J., & Lin, W. (2012). Coercing bisphosphonates to kill cancer cells with nanoscale coordination polymers. *Chemical Communications, 48*(21), 2668–2670.

Liu, D., Poon, C., Lu, K., He, C., & Lin, W. (2014a). Self-assembled nanoscale coordination polymers with trigger release properties for effective anticancer therapy. *Nature Communications, 5*(1), 1–11.

Liu, D., He, C., Poon, C., & Lin, W. (2014b). Theranostic nanoscale coordination polymers for magnetic resonance imaging and bisphosphonate delivery. *Journal of Materials Chemistry B, 2*(46), 8249–8255.

Liu, J., Zhang, L., Lei, J., Shen, H., & Ju, H. (2017). Multifunctional metal-organic framework nanoprobe for cathepsin B-activated cancer cell imaging and chemo-photodynamic therapy. *ACS Applied Materials & Interfaces, 9*(3), 2150–2158.

Liu, B., Hu, F., Zhang, J., Wang, C., & Li, L. (2019). A biomimetic coordination nanoplatform for controlled encapsulation and delivery of drug-gene combinations. *Angewandte Chemie, 131*(26), 8896–8900.

Liu, X., Jin, Y., Liu, T., Yang, S., Zhou, M., Wang, W., & Yu, H. (2020). Iron-based theranostic nanoplatform for improving chemodynamic therapy of cancer. *ACS Biomaterials Science & Engineering, 6*(9), 4834–4845.

Lu, W., Wei, Z., Gu, Z. Y., Liu, T. F., Park, J., Park, J., Tian, J., Zhang, M., Zhang, Q., Gentle, T., III, & Bosch, M. (2014). Tuning the structure and function of metal-organic frameworks via linker design. *Chemical Society Reviews, 43*(16), 5561–5593.

Lu, K., Aung, T., Guo, N., Weichselbaum, R., & Lin, W. (2018). Nanoscale metal-organic frameworks for therapeutic, imaging, and sensing applications. *Advanced Materials, 30*(37), 1707634.

Luo, Z., Fan, S., Gu, C., Liu, W., Chen, J., Li, B., & Liu, J. (2019). Metal-organic framework (MOF)-based nanomaterials for biomedical applications. *Current Medicinal Chemistry, 26*(18), 3341–3369.

Ma, B., Wang, S., Liu, F., Zhang, S., Duan, J., Li, Z., Kong, Y., Sang, Y., Liu, H., Bu, W., & Li, L. (2018). Self-assembled copper–amino acid nanoparticles for in situ glutathione "and" H_2O_2 sequentially triggered chemodynamic therapy. *Journal of the American Chemical Society, 141*(2), 849–857.

Martinez Joaristi, A., Juan-Alcañiz, J., Serra-Crespo, P., Kapteijn, F., & Gascon, J. (2012). Electrochemical synthesis of some archetypical Zn^{2+}, Cu^{2+}, and Al^{3+} metal organic frameworks. *Crystal Growth & Design, 12*(7), 3489–3498.

Meek, S. T., Greathouse, J. A., & Allendorf, M. D. (2011). Metal-organic frameworks: A rapidly growing class of versatile nanoporous materials. *Advanced Materials, 23*(2), 249–267.

Meng, Z., Huang, H., Huang, D., Zhang, F., & Mi, P. (2020). Functional metal-organic framework-based nanocarriers for accurate magnetic resonance imaging and effective eradication of breast tumor and lung metastasis. *Journal of Colloid and Interface Science, 581*, 31–43.

Mi, P., Cabral, H., & Kataoka, K. (2020). Ligand-installed nanocarriers toward precision therapy. *Advanced Materials, 32*(13), 1902604.

Mir, M., Ishtiaq, S., Rabia, S., Khatoon, M., Zeb, A., Khan, G. M., Ur Rehman, A., & Ud Din, F. (2017). Nanotechnology: From in vivo imaging system to controlled drug delivery. *Nanoscale Research Letters, 12*(1), 500.

Mueller, U., Puetter, H., Hesse, M., & Wessel, H. (2007). WO 2005/049892, 2005. *BASF Aktiengesellschaft*.

Naseri, N., Ajorlou, E., Asghari, F., & Pilehvar-Soltanahmadi, Y. (2018). An update on nanoparticle-based contrast agents in medical imaging. *Artificial Cells, Nanomedicine, and Biotechnology, 46*(6), 1111–1121.

Nejadshafiee, V., Naeimi, H., Goliaei, B., Bigdeli, B., Sadighi, A., Dehghani, S., Lotfabadi, A., Hosseini, M., Nezamtaheri, M. S., Amanlou, M., & Sharifzadeh, M. (2019). Magnetic bio-metal–organic framework nanocomposites decorated with folic acid conjugated chitosan as a promising biocompatible targeted theranostic system for cancer treatment. *Materials Science and Engineering: C, 99*, 805–815.

Nune, S. K., Gunda, P., Thallapally, P. K., Lin, Y. Y., Laird Forrest, M., & Berkland, C. J. (2009). Nanoparticles for biomedical imaging. *Expert Opinion on Drug Delivery, 6*(11), 1175–1194.

Osterrieth, J. W., & Fairen-Jimenez, D. (2020). Metal-organic framework composites for theragnostics and drug delivery applications. *Biotechnology Journal, 16*(2), 2000005.

Pan, Y. B., Wang, S., He, X., Tang, W., Wang, J., Shao, A., & Zhang, J. (2019). A combination of glioma in vivo imaging and in vivo drug delivery by metal-organic framework based composite nanoparticles. *Journal of Materials Chemistry B, 7*(48), 7683–7689.

Pandey, A., Dhas, N., Deshmukh, P., Caro, C., Patil, P., García-Martín, M. L., Padya, B., Nikam, A., Mehta, T., & Mutalik, S. (2020). Heterogeneous surface architectured metal-organic frameworks for cancer therapy, imaging, and biosensing: A state-of-the-art review. *Coordination Chemistry Reviews, 409*, 213212.

Park, K. S., Ni, Z., Côté, A. P., Choi, J. Y., Huang, R., Uribe-Romo, F. J., Chae, H. K., O'Keeffe, M., & Yaghi, O. M. (2006). Exceptional chemical and thermal stability of zeolitic imidazolate frameworks. *Proceedings of the National Academy of Sciences, 103*(27), 10186–10191.

Peer, D., Karp, J. M., Hong, S., Farokhzad, O. C., Margalit, R., & Langer, R. (2007). Nanocarriers as an emerging platform for cancer therapy. *Nature Nanotechnology, 2*(12), 751–760.

Peller, M., Böll, K., Zimpel, A., & Wuttke, S. (2018). Metal-organic framework nanoparticles for magnetic resonance imaging. *Inorganic Chemistry Frontiers, 5*(8), 1760–1779.

Pereira, G. A., Peters, J. A., Almeida Paz, F. A., Rocha, J., & Geraldes, C. F. (2010). Evaluation of [Ln (H_2cmp)(H_2O)] metal organic framework materials for potential application as magnetic resonance imaging contrast agents. *Inorganic Chemistry, 49*(6), 2969–2974.

Petros, R. A., & DeSimone, J. M. (2010). Strategies in the design of nanoparticles for therapeutic applications. *Nature Reviews Drug Dscovery, 9*(8), 615–627.

Pichon, A., Lazuen-Garay, A., & James, S. L. (2006). Solvent-free synthesis of a microporous metal-organic framework. *CrystEngComm, 8*(3), 211–214.

Qian, J., Sun, F., & Qin, L. (2012). Hydrothermal synthesis of zeolitic imidazolate framework-67 (ZIF-67) nanocrystals. *Materials Letters, 82*, 220–223.

Qian, C. G., Chen, Y. L., Feng, P. J., Xiao, X. Z., Dong, M., Yu, J. C., Hu, Q. Y., Shen, Q. D., & Gu, Z. (2017). Conjugated polymer nanomaterials for theranostics. *Acta Pharmacologica Sinica, 38*(6), 764–781.

Rieter, W. J., Pott, K. M., Taylor, K. M., & Lin, W. (2008). Nanoscale coordination polymers for platinum-based anticancer drug delivery. *Journal of the American Chemical Society, 130*(35), 11584–11585.

Robison, L., Zhang, L., Drout, R. J., Li, P., Haney, C. R., Brikha, A., Noh, H., Mehdi, B. L., Browning, N. D., Dravid, V. P., & Cui, Q. (2019). A bismuth metal-organic framework as a contrast agent for X-ray computed tomography. *ACS Applied Bio Materials, 2*(3), 1197–1203.

Rojas, S., Devic, T., & Horcajada, P. (2017). Metal organic frameworks based on bioactive components. *Journal of Materials Chemistry B, 5*(14), 2560–2573.

Rowe, M. D., Thamm, D. H., Kraft, S. L., & Boyes, S. G. (2009). Polymer-modified gadolinium metal-organic framework nanoparticles used as multifunctional nanomedicines for the targeted imaging and treatment of cancer. *Biomacromolecules, 10*(4), 983–993.

Rowsell, J. L., & Yaghi, O. M. (2004). Metal-organic frameworks: A new class of porous materials. *Microporous and Mesoporous Materials, 73*(1–2), 3–14.

Ruyra, À., Yazdi, A., Espín, J., Carné-Sánchez, A., Roher, N., Lorenzo, J., Imaz, I., & Maspoch, D. (2015). Synthesis, culture medium stability, and in vitro and in vivo zebrafish embryo toxicity of metal-organic framework nanoparticles. *Chemistry–A European Journal, 21*(6), 2508–2518.

Safaei, M., Foroughi, M. M., Ebrahimpoor, N., Jahani, S., Omidi, A., & Khatami, M. (2019). A review on metal-organic frameworks: Synthesis and applications. *TrAC Trends in Analytical Chemistry, 118*, 401–425.

Shang, W., Kang, X., Ning, H., Zhang, J., Zhang, X., Wu, Z., Mo, G., Xing, X., & Han, B. (2013). Shape and size-controlled synthesis of MOF nanocrystals with the assistance of ionic liquid mircoemulsions. *Langmuir, 29*(43), 13168–13174.

Shang, W., Zeng, C., Du, Y., Hui, H., Liang, X., Chi, C., Wang, K., Wang, Z., & Tian, J. (2017). Core-shell gold Nanorod@metal-organic framework nanoprobes for multimodality diagnosis of glioma. *Advanced Materials, 29*(3), 1604381.

Shekhah, O. (2010). Layer-by-layer method for the synthesis and growth of surface mounted metal-organic frameworks (SURMOFs). *Materials, 3*(2), 1302–1315.

Shekhah, O., Wang, H., Kowarik, S., Schreiber, F., Paulus, M., Tolan, M., Sternemann, C., Evers, F., Zacher, D., Fischer, R. A., & Wöll, C. (2007). Step-by-step route for the synthesis of metal-organic frameworks. *Journal of the American Chemical Society, 129*(49), 15118–15119.

Shekhah, O., Wang, H., Zacher, D., Fischer, R. A., & Wöll, C. (2009). Growth mechanism of metal-organic frameworks: Insights into the nucleation by employing a step-by-step route. *Angewandte Chemie International Edition, 48*(27), 5038–5041.

Shi, J., Kantoff, P. W., Wooster, R., & Farokhzad, O. C. (2017). Cancer nanomedicine: Progress, challenges and opportunities. *Nature Reviews Cancer, 17*(1), 20.

Singh, R., & Lillard, J. W. (2009). Nanoparticle-based targeted drug delivery. *Experimental and Molecular Pathology, 86*(3), 215–223.

So, M. C., Jin, S., Son, H. J., Wiederrecht, G. P., Farha, O. K., & Hupp, J. T. (2013). Layer-by-layer fabrication of oriented porous thin films based on porphyrin-containing metal–organic frameworks. *Journal of the American Chemical Society, 135*(42), 15698–15701.

Son, W. J., Kim, J., Kim, J., & Ahn, W. S. (2008). Sonochemical synthesis of MOF-5. *Chemical Communications, 47*, 6336–6338.

Sousa, D., Ferreira, D., Rodrigues, J. L., & Rodrigues, L. R. (2019). Nanotechnology in targeted drug delivery and therapeutics. In *Applications of targeted nano drugs and delivery systems* (pp. 357–409). Elsevier.

Stassen, I., Styles, M., Van Assche, T., Campagnol, N., Fransaer, J., Denayer, J., Tan, J. C., Falcaro, P., De Vos, D., & Ameloot, R. (2015). Electrochemical film deposition of the zirconium metal–organic framework UiO-66 and application in a miniaturized sorbent trap. *Chemistry of Materials, 27*(5), 1801–1807.

Stock, N., & Biswas, S. (2012). Synthesis of metal-organic frameworks (MOFs): Routes to various MOF topologies, morphologies, and composites. *Chemical Reviews, 112*(2), 933–969.

Sun, C. Y., Qin, C., Wang, X. L., & Su, Z. M. (2013). Metal-organic frameworks as potential drug delivery systems. *Expert Opinion on Drug Delivery, 10*(1), 89–101.

Sun, W., Zhai, X., & Zhao, L. (2016). Synthesis of ZIF-8 and ZIF-67 nanocrystals with well-controllable size distribution through reverse microemulsions. *Chemical Engineering Journal, 289*, 59–64.

Sun, J., Yu, X., Zhao, S., Chen, H., Tao, K., & Han, L. (2020). Solvent-controlled morphology of amino-functionalized bimetal metal-organic frameworks for asymmetric supercapacitors. *Inorganic Chemistry, 59*(16), 11385–11395.

Suslick, K. S., Hammerton, D. A., & Cline, R. E. (1986). Sonochemical hot spot. *Journal of the American Chemical Society, 108*(18), 5641–5642.

Taylor, K. M., Rieter, W. J., & Lin, W. (2008). Manganese-based nanoscale metal-organic frameworks for magnetic resonance imaging. *Journal of the American Chemical Society, 130*(44), 14358–14359.

Taylor-Pashow, K. M., Della Rocca, J., Xie, Z., Tran, S., & Lin, W. (2009). Postsynthetic modifications of iron-carboxylate nanoscale metal-organic frameworks for imaging and drug delivery. *Journal of the American Chemical Society, 131*(40), 14261–14263.

Tian, C., Zhu, L., Lin, F., & Boyes, S. G. (2015). Poly (acrylic acid) bridged gadolinium metal-organic framework-gold nanoparticle composites as contrast agents for computed tomography and magnetic resonance bimodal imaging. *ACS Applied Materials & Interfaces, 7*(32), 17765–17775.

Tranchemontagne, D. J., Hunt, J. R., & Yaghi, O. M. (2008). Room temperature synthesis of metal-organic frameworks: MOF-5, MOF-74, MOF-177, MOF-199, and IRMOF-0. *Tetrahedron, 64*(36), 8553–8557.

Wang, Q., & Astruc, D. (2019). State of the art and prospects in metal-organic framework (MOF)-based and MOF-derived nanocatalysis. *Chemical Reviews, 120*(2), 1438–1511.

Wang, D., Zhou, J., Chen, R., Shi, R., Zhao, G., Xia, G., Li, R., Liu, Z., Tian, J., Wang, H., & Guo, Z. (2016). Controllable synthesis of dual-MOFs nanostructures for pH-responsive artemisinin delivery, magnetic resonance and optical dual-model imaging-guided chemo/photothermal combinational cancer therapy. *Biomaterials, 100*, 27–40.

Wang, L., Zheng, M., & Xie, Z. (2018a). Nanoscale metal-organic frameworks for drug delivery: A conventional platform with new promise. *Journal of Materials Chemistry B, 6*(5), 707–717.

Wang, D., Wu, H., Zhou, J., Xu, P., Wang, C., Shi, R., Wang, H., Wang, H., Guo, Z., & Chen, Q. (2018b). In situ one-pot synthesis of MOF-Polydopamine hybrid Nanogels with enhanced Photothermal effect for targeted Cancer therapy. *Advanced Science, 5*(6), 1800287.

Wang, X., Yang, N., Li, Q., He, F., Yang, Y., Wu, B., Chu, J., Zhou, A., & Xiong, S. (2019a). Solvothermal synthesis of flower-string-like NiCo-MOF/MWCNT composites as a high-performance supercapacitor electrode material. *Journal of Solid State Chemistry, 277*, 575–586.

Wang, L., Qu, X., Zhao, Y., Weng, Y., Waterhouse, G. I., Yan, H., Guan, S., & Zhou, S. (2019b). Exploiting single atom iron centers in a porphyrin-like MOF for efficient cancer phototherapy. *ACS Applied Materials & Interfaces, 11*(38), 35228–35237.

Wang, Z., Li, Z., Ng, M., & Milner, P. J. (2020). Rapid mechanochemical synthesis of metal-organic frameworks using exogenous organic base. *Dalton Transactions, 49*(45), 16238–16244. https://doi.org/10.1039/D0DT01240H

Wei, R., Chi, H. Y., Li, X., Lu, D., Wan, Y., Yang, C. W., & Lai, Z. (2020). Aqueously cathodic deposition of ZIF-8 membranes for superior propylene/propane separation. *Advanced Functional Materials, 30*(7), 1907089.

Wu, M. X., & Yang, Y. W. (2017). Metal-organic framework (MOF)-based drug/cargo delivery and cancer therapy. *Advanced Materials, 29*(23), 1606134.

Xiao, Y., Wu, Z., Zhang, Q., Li, P., Yu, H., & Lu, G. (2020). Oxygen-assisted cathodic deposition of copper-carboxylate metal–organic framework films. *Crystal Growth & Design, 20*(6), 3997–4004.

Xie, J., Lee, S., & Chen, X. (2010). Nanoparticle-based theranostic agents. *Advanced Drug Delivery Reviews, 62*(11), 1064–1079.

Xue, D. X., Wang, Q., & Bai, J. (2019a). Amide-functionalized metal-organic frameworks: Syntheses, structures and improved gas storage and separation properties. *Coordination Chemistry Reviews, 378*, 2–16.

Xue, Y., Zheng, S., Xue, H., & Pang, H. (2019b). Metal-organic framework composites and their electrochemical applications. *Journal of Materials Chemistry A, 7*(13), 7301–7327.

Yaghi, O. M., & Li, H. (1995). Hydrothermal synthesis of a metal-organic framework containing large rectangular channels. *Journal of the American Chemical Society, 117*(41), 10401–10402.

Yaghi, O. M., Li, H., Davis, C., Richardson, D., & Groy, T. L. (1998). Synthetic strategies, structure patterns, and emerging properties in the chemistry of modular porous solids. *Accounts of Chemical Research, 31*(8), 474–484.

Yang, J., & Yang, Y. W. (2020). Metal-organic frameworks for biomedical applications. *Small, 16*(10), 1906846.

Yang, C., Chen, K., Chen, M., Hu, X., Huan, S. Y., Chen, L., Song, G., & Zhang, X. B. (2019). Nanoscale metal-organic framework based two-photon sensing platform for bioimaging in live tissue. *Analytical Chemistry, 91*(4), 2727–2733.

Ye, R., Ni, M., Xu, Y., Chen, H., & Li, S. (2018). Synthesis of Zn-based metal-organic frameworks in ionic liquid microemulsions at room temperature. *RSC Advances, 8*(46), 26237–26242.

Yoo, D., Lee, J. H., Shin, T. H., & Cheon, J. (2011). Theranostic magnetic nanoparticles. *Accounts of Chemical Research, 44*(10), 863–874.

Yuan, Q., & Zhu, G. (2020). A review on metal organic frameworks (MOFs) modified membrane for remediation of water pollution. *Environmental Engineering Research, 26*(3), 190435.

Zacher, D., Shekhah, O., Wöll, C., & Fischer, R. A. (2009). Thin films of metal-organic frameworks. *Chemical Society Reviews, 38*(5), 1418–1429.

Zhang, Y. B., Furukawa, H., Ko, N., Nie, W., Park, H. J., Okajima, S., Cordova, K. E., Deng, H., Kim, J., & Yaghi, O. M. (2015). Introduction of functionality, selection of topology, and enhancement of gas adsorption in multivariate metal-organic framework-177. *Journal of the American Chemical Society, 137*(7), 2641–2650.

Zhang, H., Shang, Y., Li, Y. H., Sun, S. K., & Yin, X. B. (2018a). Smart metal-organic framework-based nanoplatforms for imaging-guided precise chemotherapy. *ACS Applied Materials & Interfaces, 11*(2), 1886–1895.

Zhang, W., Lu, J., Gao, X., Li, P., Zhang, W., Ma, Y., Wang, H., & Tang, B. (2018b). Enhanced photodynamic therapy by reduced levels of intracellular glutathione obtained by employing a Nano-MOF with Cu(II) as the active center. *Angewandte Chemie, 130*(18), 4985–4990.

Zhang, S., Pei, X., Gao, H., Chen, S., & Wang, J. (2020). Metal-organic framework-based nanomaterials for biomedical applications. *Chinese Chemical Letters, 31*(5), 1060–1070.

Zhao, H. X., Zou, Q., Sun, S. K., Yu, C., Zhang, X., Li, R. J., & Fu, Y. Y. (2016). Theranostic metal-organic framework core-shell composites for magnetic resonance imaging and drug delivery. *Chemical Science, 7*(8), 5294–5301.

Zhao, J., Yang, Y., Han, X., Liang, C., Liu, J., Song, X., Ge, Z., & Liu, Z. (2017). Redox-sensitive nanoscale coordination polymers for drug delivery and cancer theranostics. *ACS Applied Materials & Interfaces, 9*(28), 23555–23563.

Zheng, W., Hao, X., Zhao, L., & Sun, W. (2017). Controllable preparation of nanoscale metal-organic frameworks by ionic liquid microemulsions. *Industrial & Engineering Chemistry Research, 56*(20), 5899–5905.

Zhou, J., Tian, G., Zeng, L., Song, X., & Bian, X. W. (2018). Nanoscaled metal-organic frameworks for biosensing, imaging, and cancer therapy. *Advanced Healthcare Materials, 7*(10), 1800022.

Zhu, H., Liu, H., Zhitomirsky, I., & Zhu, S. (2015). Preparation of metal-organic framework films by electrophoretic deposition method. *Materials Letters, 142*, 19–22.

Zhu, Y. D., Chen, S. P., Zhao, H., Yang, Y., Chen, X. Q., Sun, J., Fan, H. S., & Zhang, X. D. (2016). PPy@MIL-100 nanoparticles as a pH-and near-IR-irradiation-responsive drug carrier for simultaneous photothermal therapy and chemotherapy of cancer cells. *ACS Applied Materials & Interfaces, 8*(50), 34209–34217.

Zhu, W., Chen, M., Liu, Y., Tian, Y., Song, Z., Song, G., & Zhang, X. (2019a). A dual factor activated metal-organic framework hybrid nanoplatform for photoacoustic imaging and synergetic photo-chemotherapy. *Nanoscale, 11*(43), 20630–20637.

Zhu, W., Yang, Y., Jin, Q., Chao, Y., Tian, L., Liu, J., Dong, Z., & Liu, Z. (2019b). Two-dimensional metal-organic-framework as a unique theranostic nano-platform for nuclear imaging and chemo-photodynamic cancer therapy. *Nano Research, 12*(6), 1307–1312.

Zhu, D., Qiao, M., Liu, J., Tao, T., & Guo, C. (2020). Engineering pristine 2D metal-organic framework nanosheets for electrocatalysis. *Journal of Materials Chemistry A, 8*(17), 8143–8170.